REPETITIVE MILD TRAUMATIC BRAIN INJURY INCREASES APP AND PHOSPHO TAU WITHIN THE HIPPOCAMPUS OF A NOVEL APP/TAU MOUSE MODEL OF ALZHEIMER'S DISEASE

by

Natalie Coschigano
A Thesis
Submitted to the
Graduate Faculty
of
George Mason University
In Partial Fulfillment of
The Requirements of the Degree
Of
Master of Arts
Psychology

Committee:

_____ Director

_____

_____

_____ Department Chairperson

_____ Program Director

_____ Dean, College of Humanities and Social Sciences

Date: _____ Summer Semester 2019
George Mason University
Fairfax, VA

Repetitive Mild Traumatic Brain Injury Increases APP and Phospho Tau within the Hippocampus of a Novel APP/Tau Mouse Model of Alzheimer's Disease

A Thesis submitted in partial fulfillment of the requirements for the degree of Master of Arts at George Mason University

by

Natalie Coschigano
Bachelor of Arts
The College of Wooster, 2017

Director: Jane Flinn, Associate Professor
George Mason University

Summer Semester 2019
George Mason University
Fairfax, VA

DEDICATION

This is dedicated to my parents Peter and Karen Coschigano, along with the many people who continue to research Alzheimer's disease and the severe effects of traumatic brain injuries.

ACKNOWLEDGEMENTS

I would like to thank so many people for the continual support of this thesis. Members of the Flinn lab who assisted in the lab and supported me throughout this whole process. I specifically want to thank Kristen Craven who was my partner in crime during this whole process. All of our RAs who assisted in our many days of running behavior, especially Fernando Barrientos and Tatiana Gervase who went above and beyond. My family who has always been there for me and continued to encourage me when things got frustrating, especially with IHC. I would like to thank my committee members Dr. Murdoch and Dr. Lewis. Lastly, I have so much appreciation for Dr. Flinn and her mentorship throughout my time at George Mason. She pushed me to attempt and develop new skills within the lab. A CHSS grant helped to support this project.

TABLE OF CONTENTS

LIST OF TABLES

LIST OF FIGURES

LIST OF ABBREVIATIONS AND SYMBOLS

Alzheimer's disease ……...…… AD
Amyloid beta ……...… Aβ
Amyloid precursor protein …… APP
Circadian Rhythm ……... CR
Glial fibrillary acidic protein …… GFAP
Hippocampus …….. HC
Infralimbic cortex …… IL
Presenilin ……. PS
Repetitive mild traumatic brain injury …….. rmTBI
Traumatic brain injury ……... TBI
Transgenic ……... Tg
Wildtype …… WT

ABSTRACT

REPETITIVE MILD TRAUMATIC BRAIN INJURY INCREASES APP AND PHOSPHO TAU WITHIN THE HIPPOCAMPUS OF A NOVEL APP/TAU MOUSE MODEL OF ALZHEIMER'S DISEASE

Natalie Coschigano, MA

George Mason University, 2019

Thesis Director: Dr. Jane Flinn, PhD

Traumatic brain injuries (TBI) are a known risk factor for Alzheimer's disease (AD). Mild TBIs are the most common and often occur during adolescence there is an increased risk of sustaining an additional TBI following the first one. The TBI/AD association thus demonstrates a need to model repetitive mild TBI (rmTBI) since rmTBIs lead to the development of tau tangles and amyloid plaques, similar to those in AD. Despite this, no study to date has assessed the impact of rmTBI during adolescence on a mouse model of AD containing both amyloid and tau. J20 (hAPP) mice were crossed with rTg4510 (TauP301L) mice to create our novel mouse model displaying both Aβ plaques and tau tangles. Mice were split into four groups: AD TBI, AD sham, wildtype (WT) TBI, and WT sham. At 8 weeks of age, the mice underwent rmTBI every other day for a total of 5 hits. Behavioral assessment of the burrowing and nesting tasks were taken at 9 weeks and 3 months. The mice were aged to 8 months when immunohistochemistry (IHC) was

performed. Behavioral testing and IHC showed that the AD mice performed worse on burrowing and nesting and also showed higher levels of APP and GFAP than WT mice in both the hippocampus and infralimbic cortex. AD TBI mice also showed significantly higher levels of both APP and phospho tau in the hippocampus than AD sham mice, consistent with other studies and confirming that rmTBI is a risk factor for AD.

INTRODUCTION

Alzheimer's disease (AD), a degenerative brain disease, is the most common form of dementia. It accounts for 60-70% of cases and is characterized by a decrease in memory (Alzheimer's Association, 2016). A total of 5.4 million Americans have been diagnosed with AD, including one in nine people over the age of 65 (Alzheimer's Association, 2016) and an estimated 44 million people worldwide (Hall & Roberson, 2012). The progression of the disease is divided into four stages: pre-dementia, early, moderate, and advanced. Pre-dementia symptoms are often mistakenly blamed on aging or stress and can develop up to eight years before a person is diagnosed with AD (Bäckman et al, 2004). Although symptoms are not the same among all individuals, some are more common. These include memory loss, confusion, problems with speaking and writing, trouble understanding visual images, poor judgment, social withdrawal, changes in mood, depression, and anxiety (Alzheimer's Association, 2016).

Alzheimer's disease can progress at different rates between individuals. Behavioral symptoms typically first begin to appear in people in their mid-60s and damage to the brain often starts ten or more years prior to this (Alzheimer's Disease Education and Referral Center, 2016). There is no definitive test that can be used to diagnose AD other than a brain autopsy following death. Common approaches to

diagnosis include medical and family history, observed changes in behavior or thinking skills, cognitive tasks, and brain imaging (Alzheimer's Association, 2016).

Aside from the cognitive symptoms, there are also neurological changes happening in the brain that begin to occur many years before symptoms appear. Some characteristics include neurofibrillary tangles, neuritic plaques, and neuron loss (Khachaturian, 1985). Tau tangles and beta-amyloid (Aβ) plaques are believed to be the main contributing factors to the degrading memory loss and other symptoms associated with AD (Alzheimer's Association, 2016). Tau tangles block transportation of essential molecules inside neurons and Aβ plaques are understood to interfere with the communication of neurons at the synaptic level (Alzheimer's Association, 2016). Tangle production is the main contributor to cell death, which accounts for the shrinkage of the brain seen as the disease progresses.

Although tau tangles are one of the main contributors to the development of AD, they are often found in normal aging adults. Tau is a neuronal protein primarily regulated by phosphorylation. The assembly and stability of microtubules are promoted by tau (Iqbal et al, 2005). Tangles can lead to the weakening of episodic memory, which is one cause of the decrease in memory as people age. In a healthy human brain, there are 6 isoforms of tau that are expressed (Noble et al, 2013). These isoforms are slightly different protein sequences that typically are created by alternative splicing. This leads to different structures which result in an altered number of phosphorylation sites (Noble et al, 2013).

The difference between tau tangles found in healthy aging adults and patients with AD, AD patients exhibit abnormally hyperphosphorylated tau, which leads to the formation of tangles with a different function due to increased number of phosphates bound. (Iqbal et al, 2005). It is thought that this hyperphosphorylation is due to an imbalance in enzymatic attachment and removal of phosphates (Noble et al, 2013). This altered tau is one of the primary causes leading to neurodegeneration and dementia. In particular, phosphorylation at specific serine-proline (SP) and threonine-proline (TP) sites are associated with a variety of neurodegenerative diseases involving tau, including AD (Steinhilb et al, 2007). Phosphorylation at these sites has not been seen in healthy adults, only those displaying neurodegeneration (Steinhilb et al, 2007). It is believed that a possible cause for the abnormal hyperphosphorylation of tau is due to a structural change (Iqbal et al, 2005). This suggests that AD is in part a direct result of tau mutations which lead to tangles of a different structure as normal tau tangles.

In healthy adults, tau accumulation is often found in the medial temporal lobe. Patients with AD show tau tangle formation beginning in the entorhinal cortex. Tau tangle progression can be broken down into 6 stages (Braak & Braak, 1991). Stages 1 and 2 consist of tangles located in the entorhinal cortex, with minimal spreading into the hippocampus (HC). During stage 3, tangles make their way into the hippocampus, and the HC becomes much more affected (Braak & Braak, 1991). Stage 4 shows heavy tangle formation of CA1 in the hippocampus and the transentorhinal layer is completely affected (Braak & Braak, 1991). Stages 5 and 6 are where the more noticeable and severe changes take place, with the most notable feature being that the isocortex is tremendously affected

(Braak & Braak, 1991). Tau tangles extend from the entorhinal cortex to most of the neocortical regions (particularly throughout the temporal, parietal, and frontal lobes). This leads to the increase in cognitive deficits.

Amyloid precursor protein (APP) is a transmembrane protein that is found in high levels in the brain. Its full physiological function is still unknown; however, some studies have suggested that it plays a role in activating cell growth via a regulated enzyme that attaches a phosphate group (Sobol et al., 2014). APP is produced in large quantities and transported to the surface of the neuron. Once there, it can be processed in a number of different ways. One reported mechanism involves proteins being broken down by α-secretase followed by γ-secretase which does not result in production of plaques (O'Brien & Wong, 2011). A different reported mechanism that results in few to no plaque production is β-secretase followed by γ-secretase, producing $A\beta_{40}$ (Wright et al, 2013). This process results in the cleavage of $A\beta_{40}$, which does not result in the production of Aβ plaques like those seen in AD (O'Brien & Wong, 2011; Wright et al, 2013). An alternative mechanism of APP processing requires internalization into a vesicle where it interacts with proteases BACE1 (also known as β-secretase) and γ-secretase. Aβ is cleaved from APP by γ-secretase, which results in the release of $A\beta_{42}$ into the extracellular space and the formation of plaques (O'Brien & Wong, 2011; Wright et al, 2013). A recent study has suggested that "normal" Aβ plays a role in innate immunity and helps to protect against infection (Moir, Lathe, & Tanzi, 2018)). Conversely, during AD this pathway is overactive, which leads to inflammation and neuron damage contributing to the development of AD (Moir, Lathe, & Tanzi, 2018).

The relationship between Aβ and tau is not fully understood, like much of AD. APP mutations lead to the production of Aβ plaque formation, and hyperphosphorylated tau creates tangles. The amyloid hypothesis states that changes in Aβ lead to alterations in tau as soluble amyloid leads to the hyperphosphorylation of tau. This causes a decrease in microtubule support, resulting in the production of tau tangles and neurodegeneration along with memory deficits (Hardy, 2002). Following tangle formation, Aβ plaques begin to accumulate. Other studies, however, suggest that instead of a serial pathway, there are actually parallel elements that converge. For example, it was shown that Aβ production and tau phosphorylation can occur simultaneously, together resulting in cell loss (Small & Duff, 2008). Another study examining the dual pathways of Aβ and tau occurring alongside each other suggested that tau phosphorylation may not be directly dependent on Aβ; with Aβ effects blocked, tau phosphorylation still occurred (Zempel et al, 2010). The details of the interactions between Aβ and tau are still under investigation.

Mouse models can be manipulated through gene mutations, surgeries, and other techniques to create specific circumstances for study. Although most cases of AD in the human population are late onset, the three main genes of study (APP, presenilin-1, and presenilin-2) are associated with early onset. This starting point allowed for investigation into the cellular progression of AD (Hall & Roberson, 2012). Understanding AD pathophysiology is continually expanding in large part due to the transgenic mouse models of AD. As more is being tested and discovered about AD, new mouse models are continuously being generated and used to study different aspects of the disease. Our

novel AD mouse model displaying both Aβ plaques and tau tangles, was created by crossing the J20 and rTg4510 mouse models (which are detailed below).

The oldest and most widely used mouse models of AD are based on the transgenic expression of human APP (hAPP) (Hall & Roberson, 2012). Most of these mouse lines contain either a mutation of the γ-secretase cleavage site or a mutation in the Aβ sequence (Hall & Roberson, 2012). The J20 mouse model of AD contains the human form of APP (hAPP), which was created by inserting 2 hAPP mutations, K595N (Swedish) and M596L (Indiana), into the rodent genome which speeds up the production of amyloid (Mucke et al, 2000). This mouse model showed impairment in behavioral testing (radial arm maze) when compared to wildtype mice (Wright et al, 2013). The deficits increased with age, in that the older the mice got, the worse they performed on testing. J20 mice also show minimal neuron loss, which is a big part of AD in humans (Ramsden et al, 2005). Another genetically modified APP mouse model, line APP23, express less Aβ plaques in the brain compared to the J20 model (Roberson, 2011). However, APP23 mice still show behavioral impairment, such as on the Morris water maze where they performed worse than wildtype mice (Roberson, 2011). They also demonstrated the development of seizures at higher frequency as Aβ levels increase, which the J20 mice did not show to the same degree (Roberson et al, 2011). PDAPP mice express human APOE3 and APOE4. However, they do not begin to show Aβ plaque formation until around 15 months of age (Hartman et al, 2002). This can be undesirable in that a lot of time must be spent waiting for the mice to reach an age where proper analysis can take place and elderly mice often exhibit a decrease in mobility, which can

make running behavioral tests a challenge. Although transgenic APP mouse models allow for further understanding of the effects of APP, they do not acknowledge tau and the large role it has on the production of human AD.

Other AD mouse models contain hyperphosphorylated tau, which leads to the production of the tangles. Although none of the mouse models fully replicate the human version of AD, they have contributed significantly to discovering pieces of the biological process. Tau only mouse models, such as rTg4510, focus solely on the ramifications of the presence of tau in the brain, even though it does not lead directly to AD. The rTg4510 mouse model expresses human tau through the P301L mutation which is paired with the Ca^{2+}-calmodulin kinase II promoter to activate the tau transgene (Spires et al, 2006). There are a few major specifics that were taken into account when creating this tau mouse model. The main goal was to produce neurofibrillary tangles along with neuron loss, which would result in memory deficits (Ramsden et al, 2005). This mouse showed tau progression that is age-dependent in that tangle development increased as the mice got older (Ramsden et al, 2005). This is similar to tau progression in humans. The JNPL3 line is another mouse model that exhibits a mutation of tau (P301L). This model displays behavioral abnormalities, along with motor deficits (Lewis et al, 2000). These mice showed a decrease in motor neurons and an increase in neurofibrillary tangles, including an effect on spinal cord (Lewis et al, 2000). Due to the extreme decrease in motor abilities, behavioral testing becomes much harder to accomplish and this loses a huge aspect of AD testing and development. The tau mouse models allow for more

translational data in terms of human tauopathy. However, this is still only half the pathologies found in AD.

Another transgenic mouse model that was created for AD is the 3xTg-AD model. This mouse line carries mutations of the APP, tau, and presenilin-1 (PS1) genes. This mouse model allowed for more translational evaluation of the human form of AD. This was the first created transgenic model that contained both Aβ plaques and tau tangles (Oddo et al, 2003). It also contains PS1 (a subunit of γ-secretase), which contributes to early-onset AD (in contrast to the majority of human AD cases that are late-onset). It is unknown what the normal functions of PS are but it has been suggested that they play a role in membrane trafficking, APP processing, and the regulation of endoplasmic reticulum calcium homeostasis including its function in the triggering of action potentials (Mattson et al, 1998). Although this mouse model contains mutations of both Aβ and tau, because it is early-onset, this makes it slightly less translational to a majority of the AD population. However, the 3xTg-AD mouse is still important for studying Aβ plaque formation and tau phosphorylation. Aβ begins to appear around 3 months of age and can be found in the HC at 6 months (Oddo et al, 2003). Tau tangles can first be detected in the hippocampus around 6 months of age and increase as the mice get older (Oddo et al, 2003). Although the 3xTg-AD mouse allows for the study of Aβ and tau side by side, it does not properly demonstrate the most common form of AD, late-onset.

We are looking to expand on the mouse models currently used for Alzheimer's research. A majority of AD mouse models focus on one pathology, either tau tangles or Aβ plaques. Our lab has recently created a mouse model that displays both pathologies

(Lippi, Smith, & Flinn, 2018). This mouse model was created by crossing J20 mice, which contain a mutated APP gene, and rTg4510 mice, which contain a mutated tau gene. This offers better translational data to the human disease than each mouse line separately. Both pathologies also present earlier (around 7 months of age) than the individual, single gene models, in addition to displaying behavioral impairments. J20/rTg4510 double transgenic mice have been shown to perform significantly worse on open field, elevated zero, Barnes maze, and forced swim tests when compared to wildtype mice (Lippi, Smith, & Flinn, 2018). The double transgenic AD mice also performed significantly worse on the "daily living" activities, burrowing and nesting (Lippi, Smith, & Flinn, 2018).

There are many risk factors that can influence the development of AD, including genetics, education, upbringing, and health. Recently, traumatic brain injury (TBI) has been found to be a risk factor for AD. TBI is the leading cause of severe disability and death in people under the age of 45 (Finnie & Blumbergs, 2002). TBI is caused by a blow to the head that ultimately leads to changes in cognitive and motor functioning (Sivanandam & Thakur, 2012). Resulting symptom changes include memory, mood, movement, and responsiveness alterations. There are several levels of TBI (mild, moderate, and severe) and they are categorized on the basis of the consciousness level (Ghajar, 2000). Most concussions fall in the mild TBI (mTBI) category. This is especially common among athletes (such as football players and boxers) and deployed soldiers. The elderly population also displays a number of repetitive TBIs due to falls. Symptoms associated with TBIs include headaches, trouble concentrating, nausea, and mood change.

The recent discoveries of brain damage among football players in particular, have brought to light the severity of TBIs and the large impact they can have on the brain.

Mild traumatic brain injuries are estimated to affect more than 6 per 1000 people a year (Blennow, Hardy, & Zetterberg, 2012). Those receiving one mTBI usually make a full neurological recovery. However, they may display some short-term memory and concentration difficulties for a brief amount of time. Moderate TBI leaves patients lethargic and severe TBI often results in a comatose state (Ghajar, 2000). Neurological damage usually does not occur immediately after the injury but instead evolves within a few hours. This is due to swelling in the brain (Ghajar, 2000). Pressure buildup caused by the brain swelling leads to an increase in brain damage. The degree of the damage depends on the severity of the injury.

There are several pathological features that are similar between TBI and AD including Aβ deposits, tau hyperphosphorylation, neurite degeneration, and synapse loss (Sivanandam & Thakur, 2012). Studies have found neurofibrillary tangles in the neocortical areas of patients suffering from TBI. Tau in AD is often in a hyperphosophorylated form, which reduces microtubule binding. Cortical tangles are a key part of AD and the tau tangles found in those with TBI are similar to these tangles. However, tangles produced from TBI are often found in superficial neocortical layers (near the site of injury), while AD tangles are located in the deeper layers (Blennow, Hardy, & Zetterberg, 2012). AD tau tangles work their way from within outward while tangles from TBI do not seem to penetrate deeper into the brain. The different locations could lead tau to have slightly altered effects on behavior. Current research has yet to

examine AD tau and TBI tau side by side (and taking into account the role Aβ has in relation to tau).

Studies have examined the effects of TBI on tau in rats by generating cortical impact injuries of varying grades, either mild, moderate, or severe (Gabbita et al., 2005). The severity of the injury was determined by the depth of the impact (deeper depth meant more severe injury). To assess the impact on cleaved tau, ELISA was used. Examining multiple brain regions, it was found that the severity of the injury can influence tau. Rats that received no hit and those that experienced a single mild TBI showed similar tau levels on both sides of the HC and cortex. Moderate TBI rats had significantly higher levels of cleaved tau on the same side as the injury in both the HC and cortex. Rats with severe TBI had even higher amounts of tau in the ipsilateral HC and cortex. It was also found that the rats exhibited increased levels of tau in the opposite side of the HC when exposed to a severe injury. This suggests that the severity of a single injury can lead to an increase in brain damage, even in regions not directly receiving the impact.

TBI also causes an accumulation of APP when axonal damage occurs. This can happen a few hours after the trauma. After APP accumulation and Aβ production, Aβ is released into the tissue. Plaque formation begins to occur around the damaged axons (Blennow, Hardy, & Zetterberg, 2012). A correlation between the severity of the TBI and Aβ accumulation has been found. Repeated TBI causes more axonal damage, which in turn leads to an increase in Aβ plaque formation. The Aβ plaque formation that is seen after TBI is also comparable to that found in AD patients (Blennow, Hardy, & Zetterberg,

2012). The difference is that plaques following TBI appear a few hours after the injury, while those found in AD patients develop slowly over a longer period of time.

Many TBI studies use mice displaying Aβ only or tau only. As previously mentioned, PDAPP mice begin to show Aβ plaque formation around 15 months of age. When exposed to a single cortical impact injury between 9 and 10 months of age, it was found that specifically in the PDAPP:E4 mice, Aβ plaque formation occurred earlier, closer to 12 and 13 months of age (Hartman et al, 2002). Another study compared a single injury versus repetitive injuries. Using 9 month old Tg2576 mice, which display Aβ, it was found that repetitive mild TBI (rmTBI) caused an increase in Aβ accumulation, whereas a single injury seemed to have no effect (Uryu et al, 2002). More recently, an experiment using an APP/PS1 mouse model was exposed to 2 TBIs at either 6 or 13 months of age. They found no differences in behavior and minimal effects to Aβ levels (Cheng et al, 2018). When exposed to TBI, mice also display increased levels of tau. Although they used C57BL/J6 mice (8-12 weeks old), one study found an increased amount of tau after mice received a moderate-severe TBI (Iliff et al, 2014). However, they did not find heightened levels of glial fibrillary acidic protein (GFAP), which is associated with inflammation (Iliff et al, 2014). Yet another study involving aged mice found that 18 month old tau mice subjected to 5 TBIs showed an escalation in tau pathology whereas the mice that received a single injury displayed no difference (Ojo et al, 2013). The 3xTG-AD mouse model was also used in a TBI study. Although this model displays early-onset AD, they found increased Aβ accumulation and tau phosphorylation after TBI (Tran et al, 2011). These previous findings have helped to

examine the effects TBI has on either Aβ or tau, but not both. Both pathologies play a vital role in AD, so only examining one give us half the information.

Research has found that TBI is a strong risk factor for AD. Although multiple studies have suggested different theories, it is still not fully understood how TBI affects AD. To further this research, we used adolescents of the recently described double transgenic AD mice developing both Aβ plaques and tau tangles. These mice also received rmTBI that includes a rotational method. Injuries occurred when the mice were adolescents to mimic when a majority of the human population receives similar injuries (playing sports or being deployed at a young age). Together, this allows for generation and analysis of more translational data as injuries occurred at a time similar to those seen in humans and the display of both brain pathologies mimic those found in human AD patients. No lab has previously studied the effects of rmTBI on adolescence in a double transgenic mouse model of AD, which makes this innovative experiment important to further research. The study will allow for a deeper understanding of how Aβ, tau, and TBI all interact.

It is important to study both the behavioral and neurological aspects of AD. Along with changes in the brain and social behaviors, people with AD begin to show a decrease in their daily living activities. This includes things such as getting dressed, making their bed, or even eating. These are things that people think of as actions that come naturally. Most people do not have to think about the simple actions that are associated with each of these activities. Similar actions are also present among rodents. To examine the effects of TBI on AD in mice, two behavioral tasks, burrowing and nesting, will be run. Both are

considered to be “daily living” activities. Mice naturally like dark, cozy environments. During burrowing, wildtype mice will remove small rocks from a tube so that they are able to sleep in it. Mice also consistently build nests when shredded paper is available to them. Previous research has found that brain lesions to the HC can cause deficits in burrowing and nesting (Deacon, 2006). It would be expected that AD and TBI would exacerbate the effects of each other, with these mice showing a decrease in the “activates of daily living.”

Aside from behavioral tests, brain imaging will also be performed. For the most beneficial results, the mice will be aged until they are 8 months old. This is to allow for the production and accumulation of Aβ plaques and tau tangles through their interaction with one another. Once the mice reached 8 months of age, they were euthanized, and their brains removed and used for immunohistochemistry (IHC). IHC is used to image the location of specific target proteins. Western blots are a commonly used brain analyses, however, IHC allows for a visual localization of the proteins of interest. We examined APP, $A\beta_{40}$, $A\beta_{42}$, phospho-tau, total tau, and glial fibrillary acidic protein (GFAP). This creates a comprehensive mapping of the multiple proteins involved in AD and how they may be influenced by TBI. Tau and Aβ are the two proteins that mainly contribute to AD. As previously mentioned, Aβ is cleaved from APP by γ-secretase. GFAP (found in mature astrocytes located in the brain) was assessed as it is a measure of inflammation (as astrocyte number increase) which is important for properly examining TBI. Brain regions of focus are the infralimbic cortex (IL) and the HC. One of the earlier areas affected by tau tangles is the HC (Braak & Braak, 1991). It is expected that high levels of both total

and phospho-tau (with phospho-tau showing a slightly higher elevation) will be present in the AD mice in the HC. However, mice receiving TBI often display tau more towards the top of the brain (around where the impact occurred). It is hypothesized that AD mice who received TBI will show an increase in tau tangles due to them appearing early in both areas, the HC and IL (where the injuries took place). Aβ plaque formation is also extremely prevalent in the HC of AD mice and it is expected that these levels will be slightly heightened in AD TBI mice.

This experiment carries high importance, in that a novel double transgenic mouse model is being used. Our mouse model will allow us to examine both AD pathologies, Aβ and tau, as they are not often displayed together. As there is little to no research on TBI and AD, we will use our novel mouse model displaying both pathologies and subject them to rmTBI. Immediately following the injuries, behavioral assessment will occur. Both behavioral tests will be repeated again at 3 months of age. Once all behavioral testing is completed, the mice will be aged to 8 months to allow for a more realistic assessment for neurological deficits. IHC will be used for the quantification and localization of AD related proteins. It is hypothesized that the AD groups will perform worse on the behavioral testing than the wildtype mice. It is also expected that the mice receiving TBI will also score lower than the sham (no TBI) mice on all behavioral tasks. It is predicted that the AD only mice will slightly underperform the TBI only mice. Finally, it is hypothesized that the AD TBI mice will perform the worst on both burrowing and nesting. The wildtype sham mice will perform the best of all 4 groups and show no deficits. For IHC, the AD TBI mice will show higher levels of tau, Aβ, APP,

and GFAP than AD sham. The AD mice will show increased levels overall of APP and GFAP compared to WT mice. The WT TBI mice will show slightly increased levels of APP and GFAP than WT sham.

This experiment is a portion of a larger project. Using the same mice, a PhD student will be collecting data from the open field maze, elevated zero maze, and Morris water maze. Open field will be used as a measure to test mobility along with anxiety. Mice displaying more anxious behavior will spend a majority of their time along the other edges of the box and less time in the center. Elevated zero is another measure of anxiety. More anxious mice will spend less time in the open arms and more time in the closed arms. Morris water maze is an important task that measures spatial memory. This is done by analyzing the distance traveled and latency to find a hidden platform. This task takes place over 7 days. She also conducted brain analyses through western blots (using the same antibodies as previously mentioned), congo red and cresyl violet staining. As previously mentioned, IHC will allow for mapping the locations of the proteins in this experiment. Western blots will allow for a proper measurement of the levels of protein present. Together, this will give us a more rounded quantification of each protein. The remaining aspect of the project will be completed by our OSCAR student. She will be running circadian rhythm (CR), which is a measure of activity. However, it has also been found that mice with AD run less but also begin running later. Using blood gathered from the mice, she will also be running ELISAs to measure melatonin levels. All together, this project will allow for a rather thorough exploration of TBI and AD, and their effects on one-another.

MATERIALS AND METHODS

Subjects

A total of 55 mice were used in this study. Twenty-five double transgenic hAPP/P301L (AD) mice were split into two groups, those that received TBI (12 mice) and those that did not and were considered sham (13 mice). 30 wildtype (WT) mice were also separated into a TBI group and a sham group (16 mice and 14 mice, respectively). Twelve transgenic tau P301L (rTg4510) female mice and six transgenic hAPP (J20) male mice were purchased from The Jacksons Laboratory for breeding at George Mason University in Krasnow Institute. Before pairing, all breeders received pellets of "Love Mash" to help increase fertility and milk production. One male J20 mouse was paired with 2 female rTg4510 mice for a 2 week period. Just before birthing, the females were separated and singly housed until the pups were weaned. Pups were weaned between 21-28 days of age. After weaning, the female mothers were returned to group-housing with other females.

Female progeny were housed in groups of 2-6, while males were housed in groups of 2-4. Rat cages were used to allow the use of a regular 'igloo' and an 'igloo' consisting of a running wheel attachment. Nylabones were also be added for chewing. Food and water was consistently available. The housing room was kept on a 12-hour light/dark cycle.

Genotyping

Through the breeding process, there were 8 possible genotypes. For the purpose of this experiment, only wildtype and double transgenic mice were used in testing. To determine the genotypes, between 11 and 21 days of age, mice had a maximum of 2 mm snipped from the ends of the tails. These tails snips were then sent to Transnetyx for genotype determination.

rmTBI

Starting at 8 weeks of age, the first rmTBI took place. With 48 hours between each round, a total of 5 consecutive TBIs occurred. Mice were first anesthetized using isoflurane until they were unresponsive to a toe pinch. Using a nose cone to keep isoflurane flowing, the mouse was positioned on the platform so that the head was directly in the path of the CCI device by placing the device on the midline of the head in front of the ears. The Leica CCI device was set to a force of 3.0 m/s and, prior to the impact, the rod was dropped to a depth of 5 mm. Once properly placed, anesthesia was removed and the mouse was struck by the CCI device. Upon impact, the platform dropped and the mouse rotated to the pad below. Immediately after the fall, a timer began to determine time to righting (standing on all four legs) and time to ambulation (walking normally). The mouse was then placed in an individual mouse cage for post-injury monitoring. After no signs of neurological damage were detected (such as hunched bodies or irregular motor movements) the mouse was placed back into its home cage where it continued to be monitored for the next few hours.

Sham mice not receiving TBI still underwent anesthesia. Once they were unresponsive, the mouse was placed directly onto the pad. Once the nose cone was removed, the timer began to measure time to righting and ambulation. The mouse was then placed in an individual mouse cage to be monitored until it was ready to be placed back into its home cage.

Behavioral Tasks

The day following TBI, the first round of behavioral testing began, around 9 weeks of age. The second round of testing occurred at 3 months of age. Behavioral testing consisted of two tasks that are used to measure "daily living" activity, burrowing and nesting. Once behavioral testing was complete, the mice were aged to 8 months where they were then euthanized to examine their brains at this later time point.

Burrowing

Mice were individually housed in mouse cages for the 17-hour (5pm – 10am) duration of the test. A hollow tube with one end closed off was filled with 250g of peashingles (small rocks). A filled tube was placed into each cage already containing normal bedding. After the mouse had the ability to interact with the tube for 2 hours, the amount of peashingles in the tube was weighed and recorded. Without adding or removing any weight, the tube was placed back into the cage. This first round of weighing occurred an hour before lights off. The next morning (a few hours after lights on), the weight of the remaining peashingles left in the tube was collected and recorded. No additional enrichment was added to the cages to allow for proper assessment of the

interactions with the peashingles. Directly following the burrowing task, the mice were assessed in the nesting task.

Nesting

Mice were individually housed in mouse cages for the 24-hour duration of the task. The mice used the same cage they used during burrowing. Once the peashingles and bedding had been disposed of, the bottom of the cage was covered with corn cob bedding. 3.5g of shredded paper was scattered around the bottom of the cage. After 24 hours, the mice were removed and placed back into their home cages. Images of the nests were taken with a number placed in the top corner. Blind scoring was completed by undergraduates who were not familiar with the test. Using a number to label the nests instead of the mouse ID helped to keep the scorers from showing bias. Nests were scored on a 1-5 scale. 1: the shredded paper appears untouched; 2: some attempt to build a nest but a majority of the shredded paper is still scattered throughout; 3: a nest was constructed using a majority of the paper but some still remains scattered around the cage; 4: a nest was constructed with very little left out; 5: all of the paper was used to build the nest.

Behavioral Data Analyses

Data for both burrowing and nesting were collected manually. Data for burrowing consisted of the weight of peashingles removed from the tube. Both the 2 hour and 24 hour time period were analyzed using a two-way, treatment by genotype, analysis of variance (ANOVA) design. Data for nesting, average nest building score on a scale of 1-5, was analyzed using a two-way, treatment by genotype, ANOVA design. Data from 9

weeks and 3 months of age were analyzed separately and later compared to see if there were any changes in behavioral deficits.

Immunohistochemistry

Upon completion of all behavioral tests, the mice were aged until they were 8 months old. At this time, the mice were euthanized, their brains removed and immediately placed on dry ice. Samples were then stored at -80°C until ready for use. The frozen tissue was cut using a cryostat to produce 30μm coronal slices. Slices were collected from the IL and HC areas of interest. Brain slices were mounted to positively charged slides, which allowed for the negatively charged tissue to attach. One slice per brain antibody was used. Once mounted on the slides, the tissue was post-fixed using 4% paraformaldehyde (PFA) for 10 minutes. The slides were washed using 0.01 M PBS 3 times, for 5 minutes each. The samples were blocked with 5% normal goat serum for 1 hour at 25°C in a closed container lined with wet paper towels. The serum was removed by gently shaking the slides and the primary antibody was added immediately, no washing took place between these steps. The antibodies were against APP (ThermoFisher), $A\beta_{40}$ (ThermoFisher), $A\beta_{42}$ (ThermoFisher), phospho-tau (abcam), total tau (ThermoFisher), and GFAP (ThermoFisher). Each antibody was properly diluted into 50 μl normal goat serum, 0.1 μl/ml, 0.0005 μl/ml, 0.00167 μl/ml, 0.0000455 μl/ml, 0.0001 μl/ml, 0.00004 μl/ml, respectively. One brain from each of the four groups was also incubated with an isotype control diluted to the proper concentration of the paired primary antibody. Antibodies APP, $A\beta_{40}$, and $A\beta_{42}$ were paired with the rabbit polyclonal isotype control (ThermoFisher). The phospho-tau antibody paired with the rabbit

monoclonal isotype control (abcam) and both the antibodies for total tau and GFAP paired with the mouse monoclonal isotype control (ThermoFisher). The use of the isotype controls was to determine background signal that does not pertain to the antibodies of interest and normalize the samples to. The tissue was incubated overnight at 4°C in the same covered container lined with wet paper towels to keep the samples from drying out.

The next morning, the primary antibodies were removed from the samples by gently shaking the slides and washed using PBS for 5 minutes, 3 times. The sections were covered with a 50 μl of the Boost detection reagent (the secondary antibody) (CellSignal) and incubated at 25°C for 30 minutes in the covered container. Slides were then washed with PBS for 5 minutes, 3 times. The DAB substrate kit (CellSignal) was applied to the tissue (40 μl) in the dark for 30 seconds. The slides were rinsed off with PBS into a waste container and then washed for 3 minutes. Slides were quickly rinsed with tap water and dipped into hematoxylin for 8 seconds before being placed into a container with tap water continually flowing for 10 minutes to wash the tissue. Sections were finally dehydrated in 70% ethanol for 1 minute, 95% ethanol for 1 minute, and 100% ethanol twice for 1 minute each. The slides were cleared in xylene twice for 1 minute each. Coverslips were mounted using DPX (mounting medium), and the slides allowed to dry overnight before imaging.

Imaging

To image, slides were placed under a light microscope and captured using the microscope camera, connected to a computer. It was set to ISO 800, 1/800 exposure, and the white balance was turned on (red = 1.2, green = 1, blue = 1.2). Using the correct

magnification (4x and 10x), multiple images were captured from both the HC and IL. ImageJ was used to measure the signals produced by the IHC analysis on 10x images similar to as described by Mizukami et al (2015). Before analysis, the image was set to 8-bit and the threshold was adjusted to Yen. To measure the protein of interest, the target area (within the HC or IL) was first outlined. Pixel size was set to measure 50 and up (to capture mostly protein and less background) and the particles were analyzed to determine the percent area covered. APP, $A\beta_{40}$, $A\beta_{42}$, phospho tau, total tau, and GFAP were all analyzed in both brain regions and the average of each protein from the four groups was calculated.

Immunohistochemistry Data Analyses

Percent area for each protein of interest was collected from both the hippocampus and infralimbic cortex. The percent area of all the brains was normalized to the paired isotype control. Any negative number was depicted as 0.001 to allow for proper analysis. Data for APP and GFAP from all four groups were analyzed using a two-way, treatment by genotype, ANOVA design. Data for $A\beta_{40}$, $A\beta_{42}$, phospho tau, and total tau from both AD groups were analyzed using an independent sample t-test.

RESULTS

25 double transgenic hAPP/P301L (AD) mice and 30 wildtype (WT) mice either received rmTBI or no injury. It was hypothesized that over all, the AD mice would perform worse on the behavioral tasks than the WT mice and that the TBI mice would perform lower (worse) than the sham mice. Of the four groups, it was hypothesized that the AD TBI mice would score the lowest, followed but the AD sham, WT TBI, and WT sham groups. It was hypothesized that the AD mice in this study would show higher levels of APP and GFAP than the WT groups with TBI being slightly higher than sham and AD TBI mice would show higher levels of some or all of APP, $A\beta_{40}$, $A\beta_{42}$, phosphor tau, total tau, and GFAP than AD sham.

Behavior

At 9 weeks of age, directly following TBI, the mice underwent the first round of behavioral testing, burrowing and nesting. In burrowing, there was a significant main effect for genotype, $F(1,47) = 51.129$, $p < 0.001$ (Figure 1). AD mice ($M = 63.732$, $SD = 9.981$) burrowed significantly less than WT mice ($M = 159.775$, $SD = 8.989$). There was no significant main effect for TBI, $F(1,47) = 0.262$, $p = 0.611$, and no significant interaction between genotype and TBI, $F(1,47) = 2.831$, $p = 0.099$.

Table 1. Average burrowing scores collected at 9 weeks. Amount of peashingles burrowed (measured in grams) were collected when the mice were 9 weeks old. Data were obtained at two time points, 2 hours and 12 hours.

	AD TBI	AD Sham	WT TBI	WT Sham
2 Hours	51.017 (*SD* = 52.873)	25.308 (*SD* = 25.961)	99.494 (*SD* = 102.423)	107.250 (*SD* = 73.704)
12 Hours	112.692 (*SD* = 64.626)	77.300 (*SD* = 42.339)	204.331 (*SD* = 41.539)	229.586 (*SD* = 25.467)

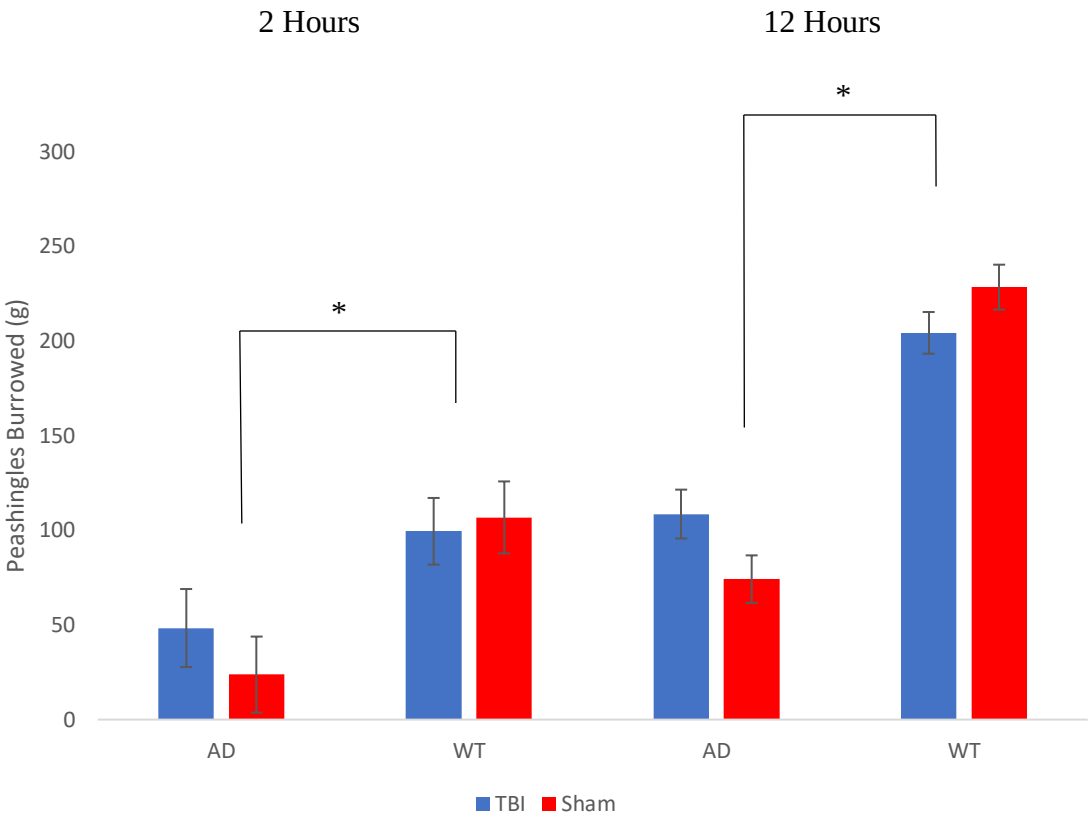

Figure 1. Burrowing scores collected at 9 weeks. Amount of peashingles burrowed (measured in grams) were collected when the mice were 9 weeks old. Data were obtained at two time points, 2 hours and 12 hours. A two-way, genotype by treatment, ANOVA was run. Error bars depict standard error. Asterisk (*) indicate $p < 0.05$. genotypes.

Nesting also showed a significant main effect for genotype, $F(1,47) = 62.160$, $p < 0.001$ (Figure 2). AD mice ($M = 2.106$, $SD = 0.201$) built worse nests than WT mice ($M = 4.240$, $SD = 0.181$). There was not a significant main effect for TBI, $F(1,47) = 0.029$, $p = 0.866$, or a significant interaction, $F(1,47) = 2.565$, $p = 0.116$.

Table 2. Average nesting score collected at 9 weeks. Average nesting score collected when the mice were 9 weeks of age. Scoring was based on a 1-5 scale: 1- shredded paper appears untouched; 2: some attempt to build a nest but a majority of the shredded paper is still scattered; 3: a nest was constructed using a majority of the paper but some still remains; 4: a nest was constructed with very little left out; 5: all of the paper was used to build the nest.

AD TBI	AD Sham	WT TBI	WT Sham
2.333 (*SD* = 0.888)	1.846 (*SD* = 1.028)	4.000 (*SD* = 1.000)	4.500 (*SD* = 0.920)

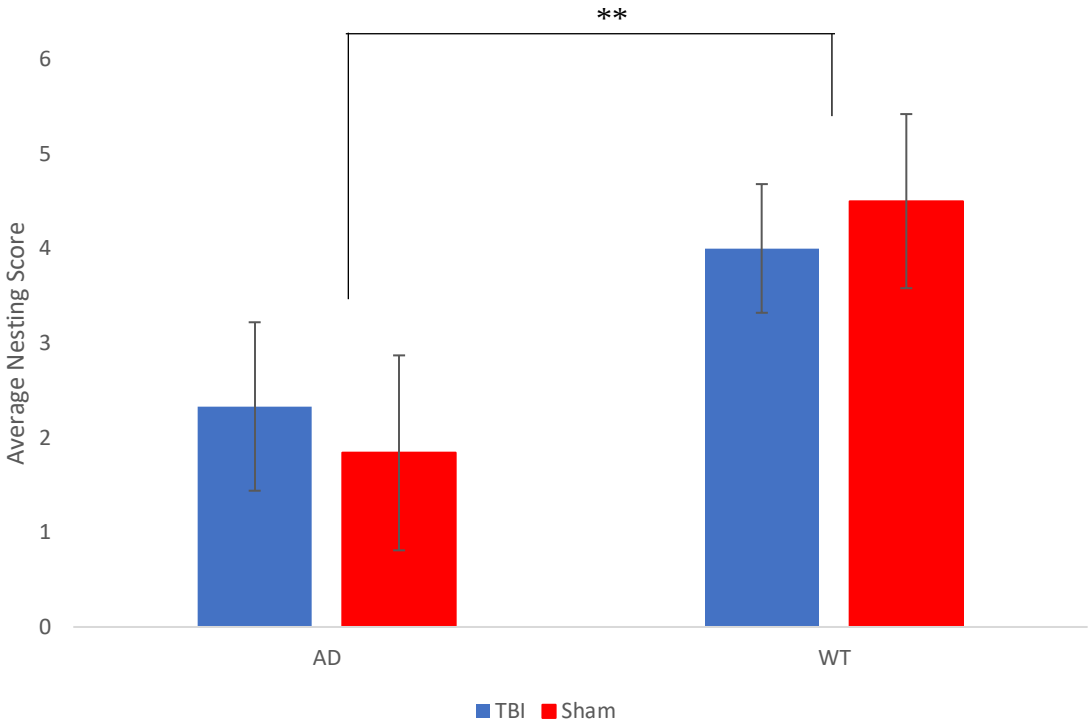

Figure 2. Nesting score collected at 9 weeks. Average nesting score collected when the mice were 9 weeks of age. Scoring was based on a 1-5 scale: 1- shredded paper appears untouched; 2: some attempt to build a nest but a majority of the shredded paper is still scattered; 3: a nest was constructed using a majority of the paper but some still remains; 4: a nest was constructed with very little left out; 5: all of the paper was used to build the nest. A two-way, genotype by treatment, ANOVA was run. Error bars depict standard error. Double asterisks (**) indicate $p < 0.001$.

The mice underwent the second round of behavioral testing at 3 months of age. Burrowing showed a significant main effect for genotype, $F(1,47) = 63.185$, $p < 0.001$ (Figure 3). AD mice ($M = 73.774$, $SD = 11.009$) burrowed less than WT mice ($M = 191.538$, $SD = 9.914$). TBI showed no significant main effect, $F(1,47) = 0.001$, $p = 0.981$, and there was no significant interaction, $F(1,47) = 0.148$, $p = 0.702$.

Table 3. Average burrowing scores collected at 3 months. Amount of peashingles burrowed (measured in grams) were collected when the mice were 3 months old. Data were obtained at two time points, 2 hours and 12 hours.

	AD TBI	AD Sham	WT TBI	WT Sham
2 Hours	50.042 (*SD* = 56.788)	43.062 (*SD* = 48.509)	149.088 (*SD* = 69.057)	160.814 (*SD* = 59.748)
12 Hours	116.425 (*SD* = 84.634)	99.823 (*SD* = 78.530)	228.644 (*SD* = 38.563)	220.229(*SD* = 52.759)

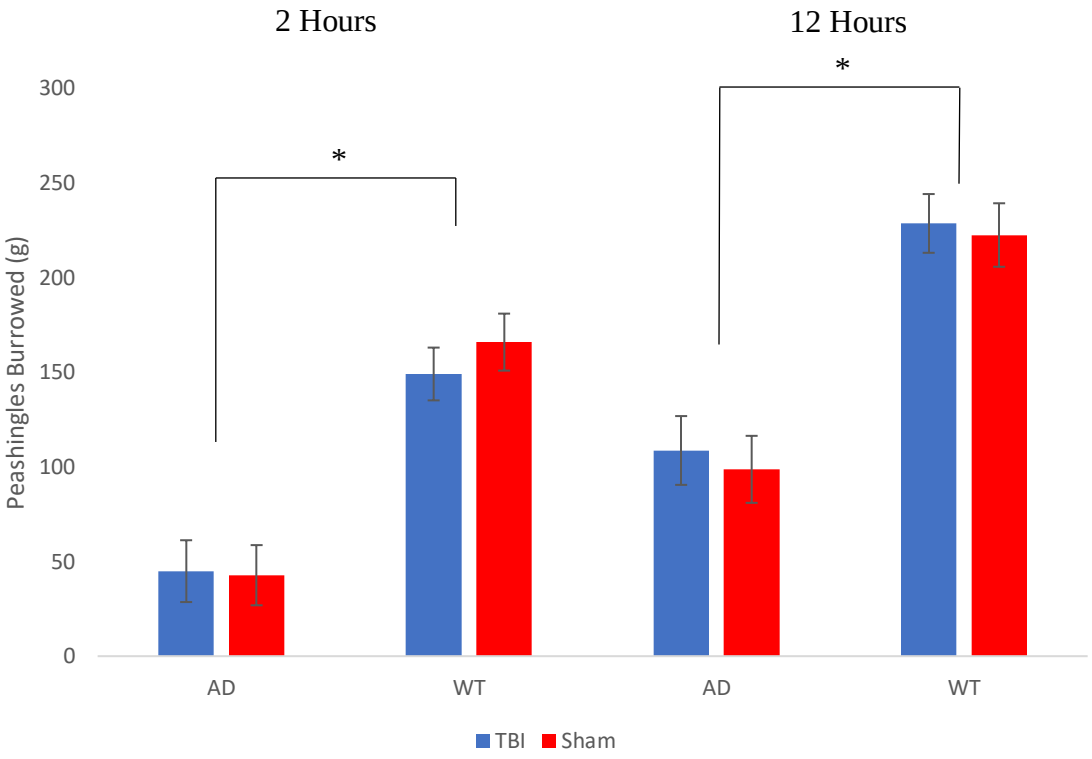

Figure 3. Burrowing scores collected at 3 months. Amount of peashingles burrowed (measured in grams) were collected when the mice reached 3 months of age. Data were obtained at two time points, 2 hours and 12 hours. A two-way, genotype by treatment, ANOVA was run. Error bars depict standard error. Asterisk (*) indicates $p < 0.05$.

Nesting once again showed a significant main effect for genotype, $F(1,47) = 52.423$, $p < 0.001$, where AD mice ($M = 2.184$, $SD = 0.203$) continued to build worse nests than WT mice ($M = 4.161$, $SD = 0.183$) (Figure 3). No significant main effect for TBI was found, $F(1,47) = 0.373$, $p = 0.545$, along with no significant interaction between genotype and TBI, $F(1,47) = 0.246$, $p = 0.622$.

Table 4. Average nesting score collected at 3 months. Average nesting score collected when the mice were 3 months of age. Scoring was based on a 1-5 scale: 1- shredded paper appears untouched; 2: some attempt to build a nest but a majority of the shredded paper is still scattered; 3: a nest was constructed using a majority of the paper but some still remains; 4: a nest was constructed with very little left out; 5: all of the paper was used to build the nest.

AD TBI	AD Sham	WT TBI	WT Sham
2.167 (*SD* = 1.135)	2.115 (*SD* = 1.064)	4.313 (*SD* = 0.574)	4.036 (*SD* = 1.082)

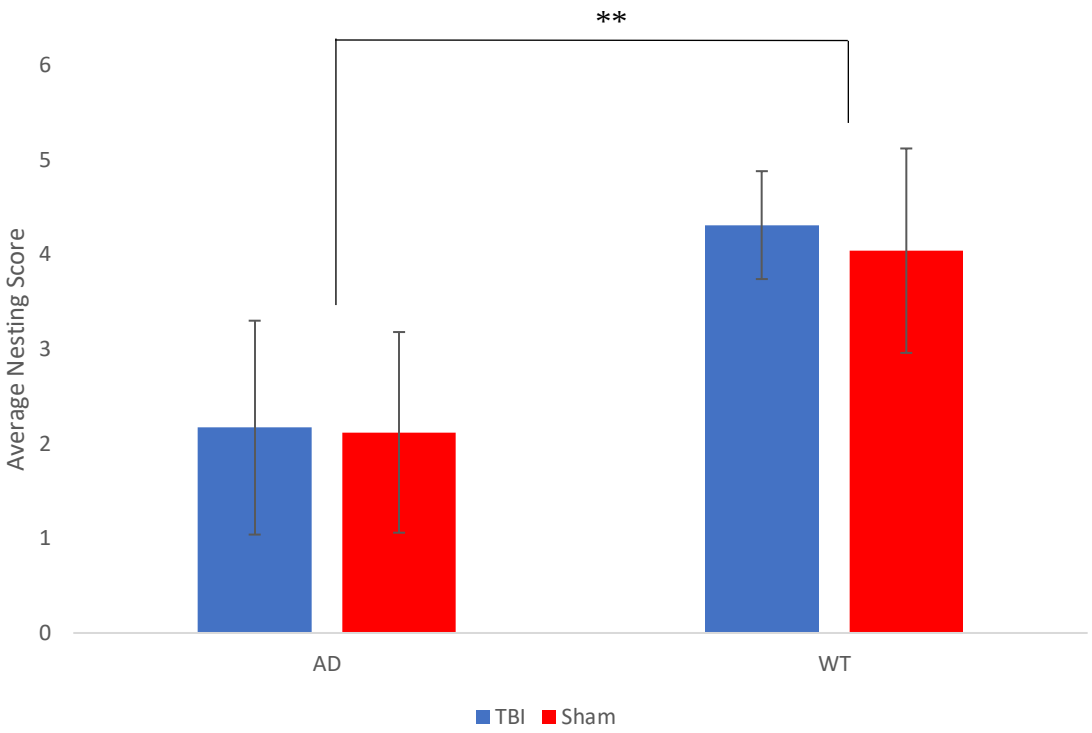

Figure 4. Nesting score collected at 3 months. Average nesting score collected when the mice were 3 months of age. Scoring was based on a 1-5 scale: 1- shredded paper appears untouched; 2: some attempt to build a nest but a majority of the shredded paper is still scattered; 3: a nest was constructed using a majority of the paper but some still remains; 4: a nest was constructed with very little left out; 5: all of the paper was used to build the nest. A two-way, genotype by treatment, ANOVA was run. Error bars depict standard error. Double asterisks (**) indicate $p < 0.001$.

Immunohistochemistry

The mice were aged to 8 months and then the brains were collected for IHC. Four brains were used for both AD groups for APP, $A\beta_{40}$, $A\beta_{42}$, phosphor tau, total tau, and GFAP antibodies and the WT groups for APP and GFAP. Slices were taken from the HC and IL. One slice per antibody per brain was used. Percent area of the target areas were measured and normalized to the paired isotype control. A previous study reported that

WT mice (including those having received TBI) do not show Aβ or tau (both phospho and total) through immunohistochemistry and western blots (Tran et al, 2011).

Within the HC, the APP antibody was measured in all four groups. A significant main effect was found for genotype, $F(1,12) = 17.185$, $p = 0.001$. AD mice ($M = 18.158$, $SD = 11.645$) showed more APP in the HC than WT mice ($M = 2.704$, $SD = 3.296$). There was no significant difference between animals receiving TBI and those that did not, $F(1,12) = 1.251$, $p = 0.285$. A significant interaction between genotype and TBI was found, $F(1,12) = 5.192$, $p = 0.042$. AD TBI mice ($M = 24.491$, $SD = 13.776$) did not show a significantly higher percent area than AD sham ($M = 11.826$. $SD = 4.439$), $p = 0.200$. AD TBI mice were significantly higher than WT TBI ($M = 0.542$, $SD = 0.678$), $p = 0.004$, and WT sham ($M = 4.866$, $SD = 3.525$), $p = 0.017$ (Table 5, Figure 5).

GFAP showed a significant main effect for genotype in the HC, $F(1,12) = 26.843$, $p < 0.001$, with AD mice ($M = 27.370$, $SD = 12.654$) showing a higher percent area than WT mice ($M = 1.551$, $SD = 4.383$) (Table 5). No significant main effect was found for TBI, $F(1,12) = 0.026$, $p = 0.876$, along with no significant interaction, $F(1,12) = 0.611$, $p = 0.450$. A breakdown of the specific means of all four groups can be found in Table 5 (Figure 5).

Table 5. Immunohistochemistry analysis of the hippocampus. Average percent area of protein present within the hippocampus normalized to the correct isotype control (as described in methods) for APP and GFAP in AD TBI, AD sham, WT TBI, and WT sham. N = 4 per group.

	AD TBI	AD Sham	WT TBI	WT Sham
APP	24.491 (*SD* = 13.776)	11.826 (*SD* = 4.439)	0.542 (*SD* = 0.678)	4.866 (*SD* = 3.525)
GFAP	25.024 (*SD* = 16.073)	29.716 (*SD* = 10.030)	0.001 (*SD* = 6.199)	0.001 (*SD* = 0.000)

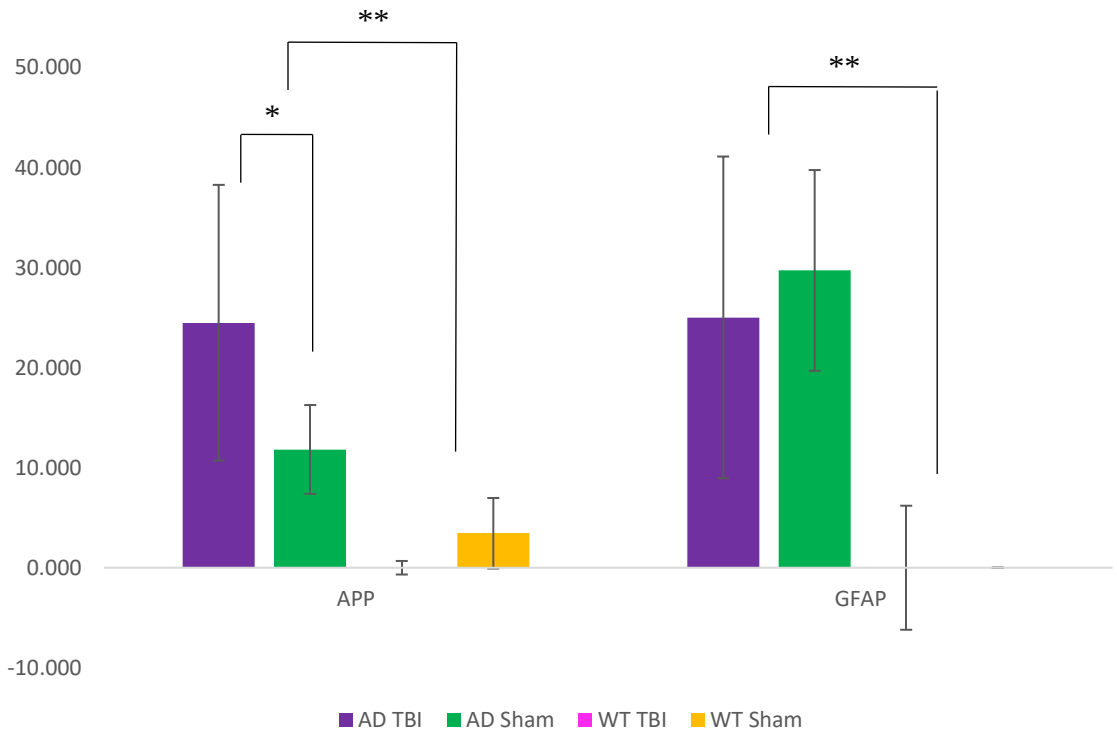

Figure 5. Immunohistochemistry analysis of the hippocampus. Average percent area of protein present within the hippocampus normalized to the correct isotype control (as described in methods) for APP and GFAP in AD TBI, AD sham, WT TBI, and WT sham. N = 4 per group. Asterisk (*) indicates $p < 0.05$ and double asterisk (**) indicates $p < 0.001$.

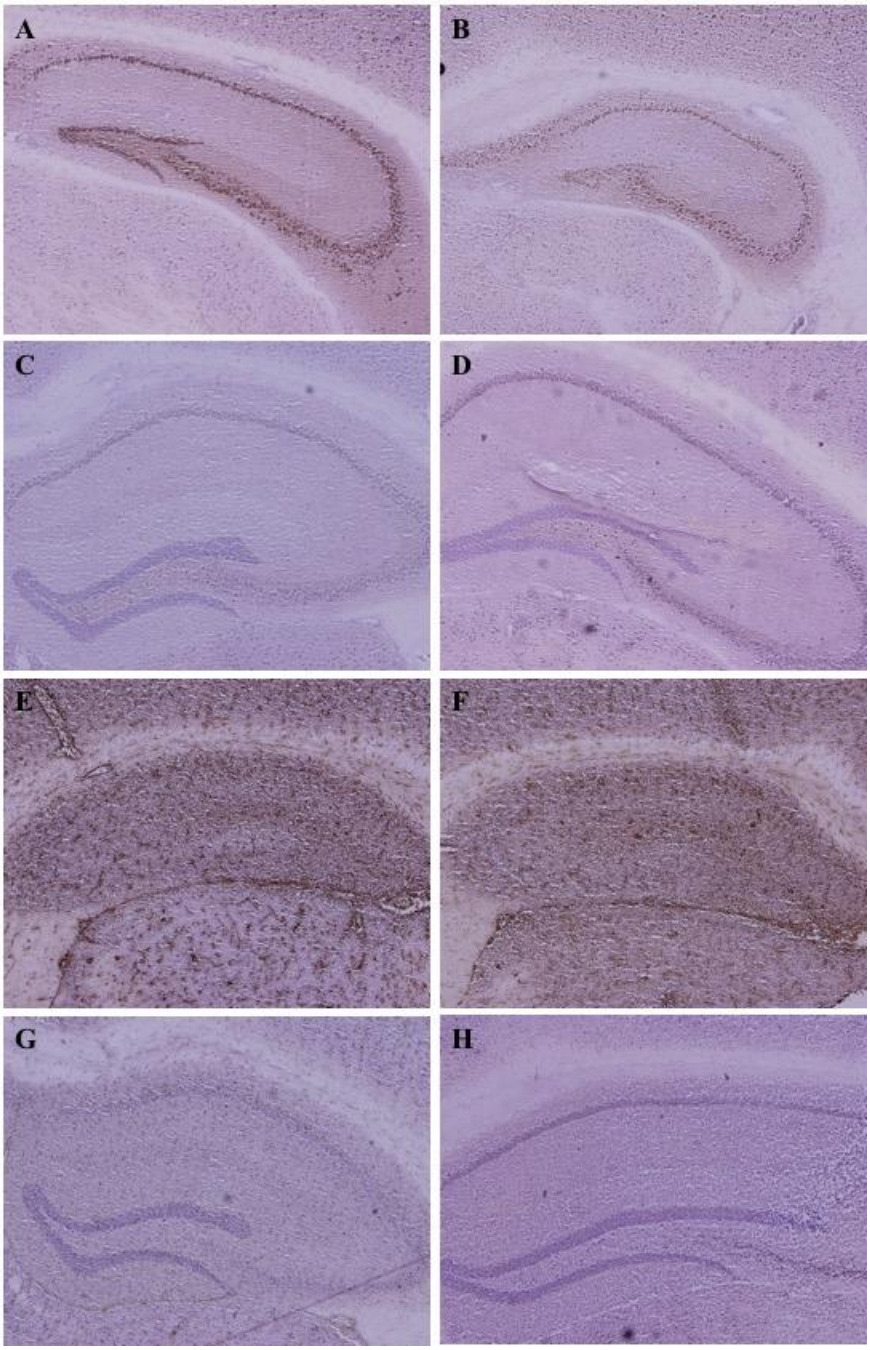

Figure 6. Immunohistochemistry imaging of the hippocampus at 4x. **A.** Example AD TBI mouse brain tagged with APP **B.** Example AD sham mouse brain tagged with APP **C.** Example WT TBI mouse brain tagged with APP **D.** Example WT sham mouse brain tagged with APP **E.** Example AD TBI mouse brain tagged with GFAP **F.** Example AD

sham mouse brain tagged with GFAP **G.** Example WT TBI mouse brain tagged with GFAP **H.** Example WT sham mouse brain tagged with GFAP

Phospho tau displayed a significant difference in percent area between AD TBI and AD sham, $t(6) = -1.772$, $p = 0.004$. AD mice that received TBI ($M = 30.712$, $SD = 25.044$) showed a higher percent of phospho tau than AD mice that did not receive TBI ($M = 7.539$, $SD = 7.543$) (Table 6, Figure 7). No significant TBI effect was found between the AD mice for $A\beta_{40}$, $t(6) = -1.512$, $p = 0.154$, and total tau, $t(6) = -1.264$, $p = 0.122$ (Table 6, Figure 7). No analysis could be run on the $A\beta_{42}$ data because there was no deviation.

Table 6. Immunohistochemistry analysis of the hippocampus. Percent area of protein present within the hippocampus normalized to the correct isotype control (as described in methods) for $A\beta_{40}$, $A\beta_{42}$, phospho tau, and total tau in both AD groups. N = 4 per group.

	AD TBI	AD Sham
$A\beta_{40}$	20.766 (*SD* = 19.590)	7.786 (*SD* = 7.735)
$A\beta_{42}$	0.001 (*SD* = 0.000)	0.001 (*SD* = 0.000)
Phospho Tau	30.712 (*SD* = 25.044)	7.539 (*SD* = 7.543
Total Tau	19.497 (*SD* = 23.328)	1.839 (*SD* = 5.340)

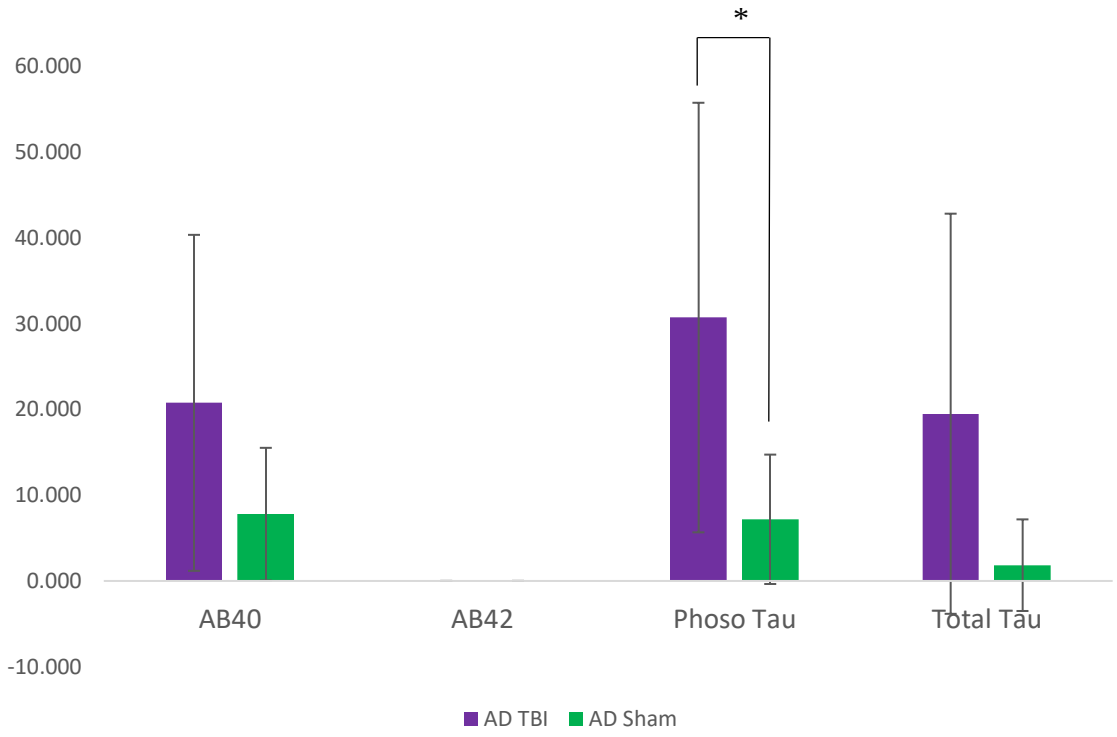

Figure 7. Immunohistochemistry analysis of the hippocampus. Percent area of protein present within the hippocampus normalized to the correct isotype control (as described in methods) for $A\beta_{40}$, $A\beta_{42}$, phospho tau, and total tau in both AD groups. N = 4 per group. Asterisk (*) indicates $p < 0.05$.

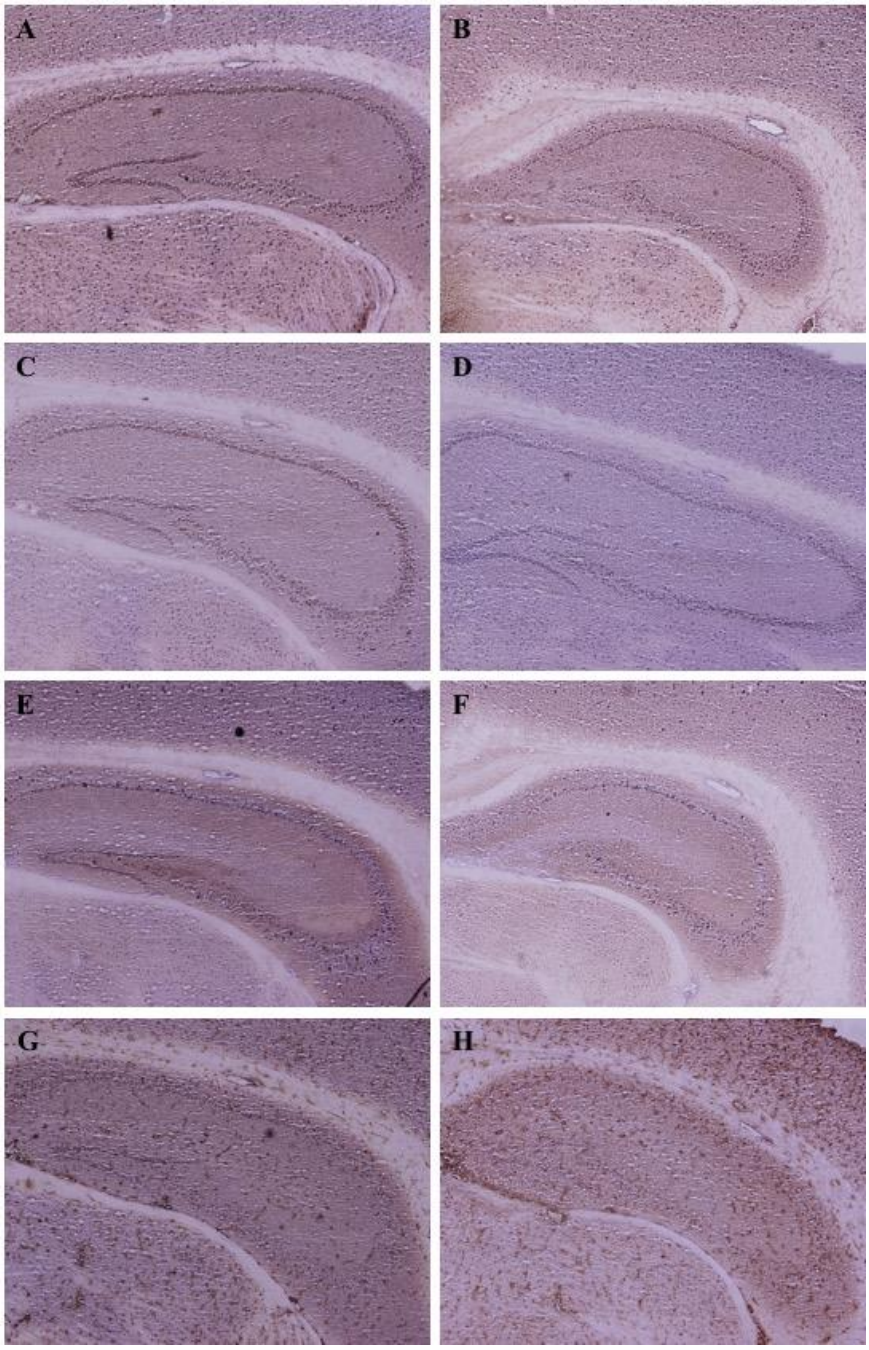

Figure 8. Immunohistochemistry imaging of the hippocampus at 4x. **A.** Example AD TBI mouse brain tagged with $A\beta_{40}$ **B.** Example AD sham mouse brain tagged with $A\beta_{40}$ **C.** Example AD TBI mouse brain tagged with $A\beta_{42}$ **D.** Example AD sham mouse brain tagged with $A\beta_{42}$ **E.** Example AD TBI mouse brain tagged with phospho tau **F.** Example AD sham mouse brain tagged with phospho tau **G.** Example AD TBI mouse brain tagged with total tau **H.** Example AD sham mouse brain tagged with total tau

Percent area of the antibodies was also measured in the IL. APP and GFAP were measured in all four groups. A significant main effect for APP was found for genotype, $F(1,12) = 5.826$, $p = 0.033$ (Table 7, Figure 9). AD mice ($M = 2.758$, $SD = 3.147$) had a significantly higher amount of APP than WT mice ($M = 0.001$, $SD = 0.000$). There was no significant main effect for TBI, $F(1,12) = 0.646$, $p = 0.437$, and no significant interaction, $F(1) = 0.646$, $p = 0.437$ (Figure 9).

Percent area of GFAP also displayed a significant main effect for genotype, $F(1,12) = 6.293$, $p = 0.027$, with AD mice ($M = 11.711$, $SD = 7.228$) showing higher levels than WT mice ($M = 3.197$, $SD = 5.975$) (Table 7, Figure 9). No significant main effect of TBI, $F(1,12) = 0.221$, $p = 0.646$, or a significant interaction, $F(1,12) = 1.139$, $p = 0.307$, was found (Figure 9).

Table 7. Immunohistochemistry analysis of the infralimbic cortex. Average percent area of protein present within the infralimbic cortex normalized to the correct isotype control (as described in methods) for APP and GFAP in AD TBI, AD sham, WT TBI, and WT sham. N = 4 per group.

	AD TBI	AD Sham	WT TBI	WT Sham
APP	3.676 (*SD* = 2.710)	0.109 (*SD* = 3.678)	0.001 (*SD* = 0.000)	0.001 (*SD* = 0.000)
GFAP	14.321 (*SD* = 8.095)	8.753 (*SD* = 6.183)	0.751 (*SD* = 3.117)	0.001 (*SD* = 8.417)

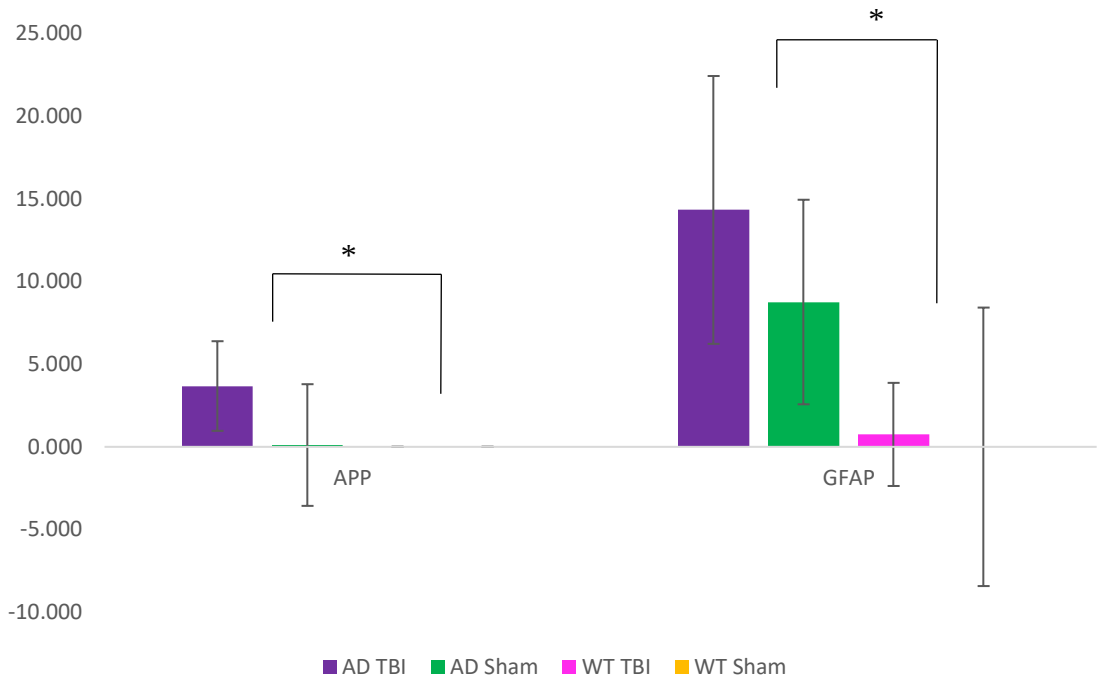

Figure 9. Immunohistochemistry analysis of the infralimbic cortex. Average percent area of protein present within the infralimbic cortex normalized to the correct isotype control (as described in methods) for APP and GFAP in AD TBI, AD sham, WT TBI, and WT sham. N = 4 per group. Asterisk (*) indicates $p < 0.05$.

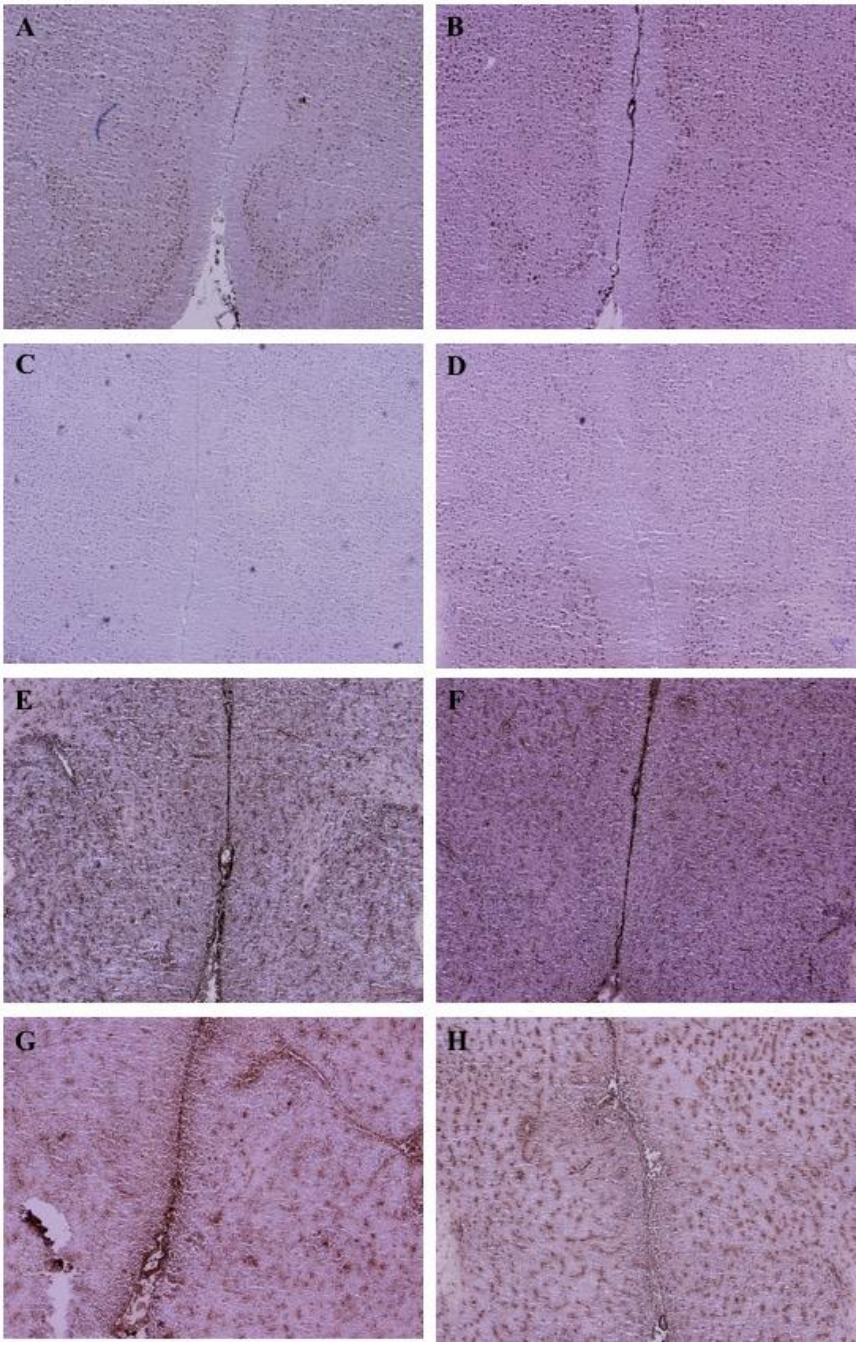

Figure 10. Immunohistochemistry imaging of the infralimbic cortex at 4x. **A.** Example AD TBI mouse brain tagged with APP **B.** Example AD sham mouse brain tagged with APP **C.** Example WT TBI mouse brain tagged with APP **D.** Example WT sham mouse brain tagged with APP **E.** Example AD TBI mouse brain tagged with GFAP **F.** Example AD sham mouse brain tagged with GFAP **G.** Example WT TBI mouse brain tagged with GFAP **H.** Example WT sham mouse brain tagged with GFAP

Within the IL, the percent area of $A\beta_{40}$, $A\beta_{42}$, phospho tau, and total tau were measured between AD TBI and AD sham. Neither $A\beta_{40}$, $t(6) = -2.092$, $p = 0.387$, nor $A\beta_{42}$, $t(6) = -2.395$, $p = 0.062$, displayed a significant difference. There was also no significance for phospho tau, $t(6) = -1.912$, $p = 0.544$, and total tau, $t(6) = -1.543$, $p = 0.988$ (Table 8, Figure 11).

Table 8. Immunohistochemistry analysis of the infralimbic cortex. Percent area of protein present within the infralimbic cortex normalized to the correct isotype control (as described in methods) for $A\beta_{40}$, $A\beta_{42}$, phospho tau, and total tau in both AD groups. N = 4 per group.

	AD TBI	AD Sham
$A\beta_{40}$	6.898 (*SD* = 4.446)	1.431 (*SD* = 2.421)
$A\beta_{42}$	15.720 (*SD* = 12.234)	0.626 (*SD* = 0.895)
Phospho Tau	8.109 (*SD* = 2.749)	1.155 (*SD* = 4.408)
Total Tau	12.812 (*SD* = 8.273)	3.172 (*SD* = 7.935)

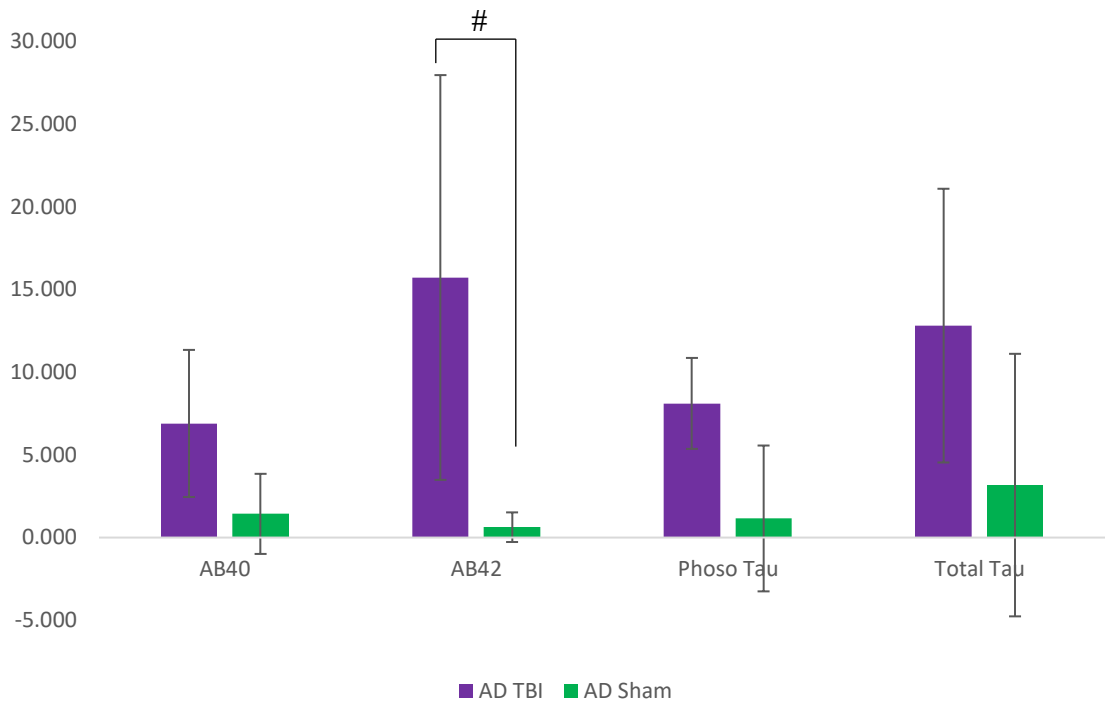

Figure 11. Immunohistochemistry analysis of the infralimbic cortex. Percent area of protein present within the infralimbic cortex normalized to the correct isotype control (as described in methods) for $A\beta_{40}$, $A\beta_{42}$, phospho tau, and total tau in both AD groups. N = 4 per group. Pound (#) indicates $p < 0.1$.

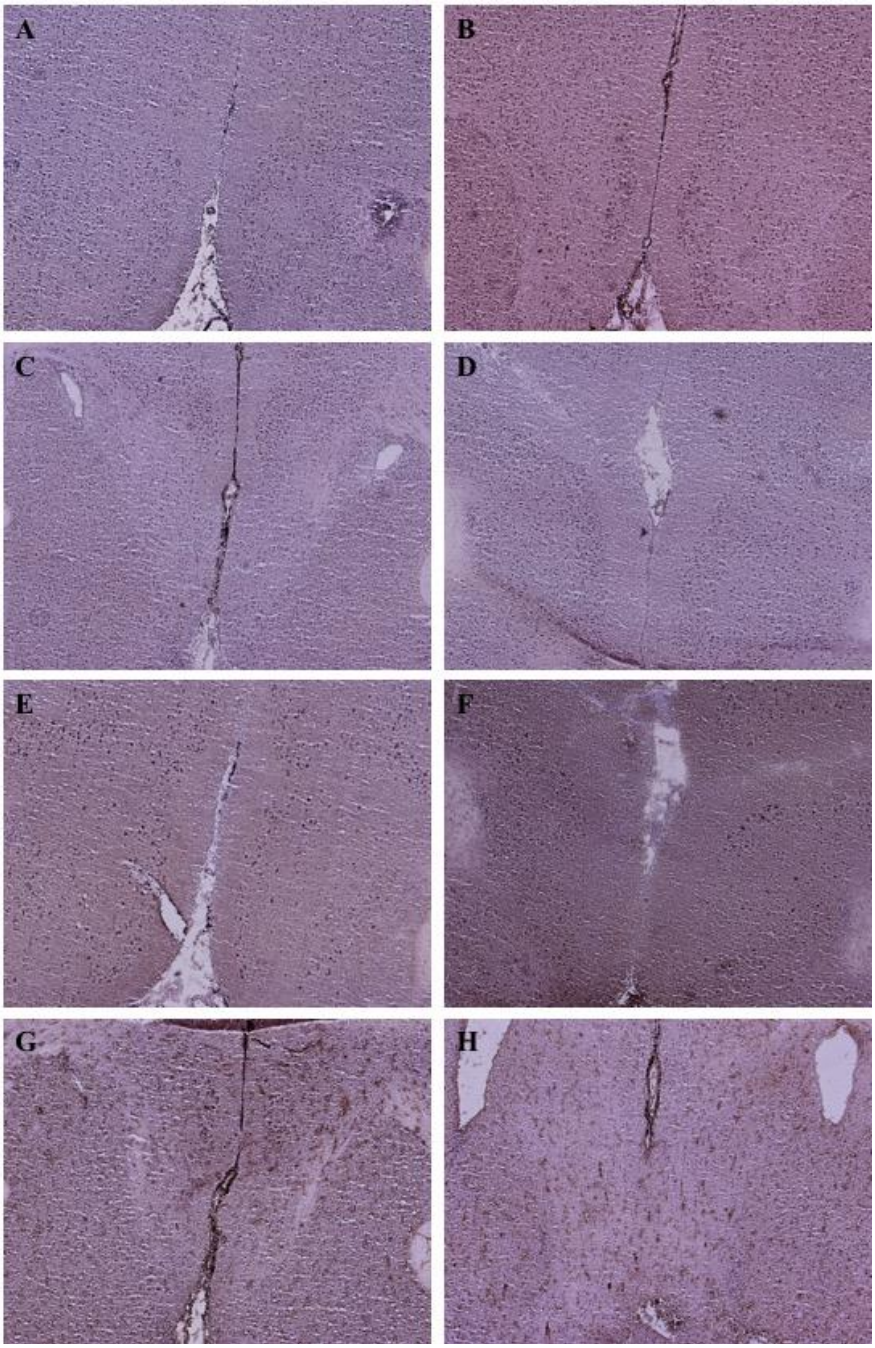

Figure 12. Immunohistochemistry imaging of the infralimbic cortex at 4x. **A.** Example AD TBI mouse brain tagged with $A\beta_{40}$ **B.** Example AD sham mouse brain tagged with $A\beta_{40}$ **C.** Example AD TBI mouse brain tagged with $A\beta_{42}$ **D.** Example AD sham mouse brain tagged with $A\beta_{42}$ **E.** Example AD TBI mouse brain tagged with phospho tau **F.** Example AD sham mouse brain tagged with phospho tau **G.** Example AD TBI mouse brain tagged with total tau **H.** Example AD sham mouse brain tagged with total tau

For APP and GFAP, the HC and IL were compared to determine if there is a difference in location between all four groups. APP showed a significant main effect for brain region, $F(1,24) = 21.558$, $p < 0.001$. The HC showed a higher percent area of APP ($M = 10.431$, $SD = 11.491$) than the IL ($M = 1.379$, $SD = 2.579$). There was a significant two-way interaction between genotype and brain region, $F(1,24) = 10.606$, $p = 0.003$. The AD mice showed significantly higher amounts of APP in the HC ($M = 18.158$, $SD = 11.645$) than the IL of AD mice ($M = 2.758$, $SD = 3.147$), $p < 0.001$, the HC of WT mice ($M = 2.704$, $SD = 3.296$), $p < 0.001$, and the IL of WT mice ($M = 0.001$, $SD = 0.000$), $p < 0.001$. There was no significant interaction for brain region and TBI, $F(1,24) = 0.696$, $p = 0.412$, or a significant three-way interaction, $F(1,24) = 3.776$, $p = 0.064$. GFAP also showed a significant main effect for brain region, $F(1,24) = 5.401$, $p = 0.029$. The HC showed a higher percent area ($M = 14.460$, $SD = 16.170$) than the IL ($M = 7.454$, $SD = 7.770$). There was also a significant interaction between genotype and brain region. The HC of AD mice showed significantly higher levels of GFAP ($M = 27.370$, $SD = 12.654$) than the IL of AD brains ($M = 11.711$, $SD = 7.228$), $p = 0.004$, the HC of WT mice ($M = 1.551$, $SD = 4.383$), $p < 0.001$, and the IL of WT mice ($M = 3.197$, $SD = 5.975$), $p < 0.001$. There was no significant interaction between brain region and TBI, $F(1,24) = 0.158$, $p = 0.695$. The three-way interaction was also not significant, $F(1,24) = 1.555$, $p = 0.224$.

$A\beta_{40}$, $A\beta_{42}$, phospho tau, and total tau were compared between brain regions for the AD groups. $A\beta_{40}$ showed no significant difference in brain regions, $F(1,12) = 4.507$, $p = 0.055$, and no significant interaction of brain region and treatment, $F(1,12) = 0.963$, p

= 0.346. $A\beta_{42}$ showed both a significant main effect for brain region, $F(1,12) = 7.459$, $p = 0.018$, and a significant interaction for brain region and TBI, $F(1,12) = 5.735$, $p = 0.034$. The AD TBI mice showed significantly higher amounts of $A\beta_{42}$ in the IL ($M = 15.720$, $SD = 12.234$) than the IL of the AD sham mice ($M = 1.032$, $SD = 0.895$), $p = 0.032$, the HC of AD TBI brains ($M = 0.001$, $SD = 0.000$), $p = 0.021$, and the HC of AD sham mice ($M = 0.001$, $SD = 0.000$), $p = 0.021$. Phospho tau showed no significant main effect for brain region, $F(1,12) = 4.100$, $p = 0.066$, or a significant interaction effect for brain region and TBI, $F(1,12) = 1.865$, p = 0.197. Total tau also showed no significant main effect for brain region, $F(1,12) = 0.351$, $p = 0.565$, or a significant interaction, $F(1,12) = 0.224$, $p = 0.644$.

DISCUSSION

The purpose of this study was to further examine a known risk factor (TBI) for AD and the effects it has on the brain and behavior in AD. TBIs are often seen in athletes, deployed soldiers, and the elderly. With mTBIs affecting more than 6 per 1000 people a year (Blennow, Hardy, & Zetterberg, 2012), it is important to understand the neurological damage occurring. Due to recent media exposure, TBI research has expanded drastically and become a highly examined topic. To properly study AD, it is important to use a model that closely displays the pathologies and behavioral symptoms found in humans. A majority of mouse models focus on either Aβ plaques or tau tangles only. The 3xTg-AD mouse model displays both but also includes PS1 (Oddo et al, 2003). This 3xTg-AD model shows similar symptoms as those found in early-onset AD. Our novel mouse model contains the human form of both Aβ plaques and tau tangles to mimic late-onset AD, as seen in the human population, but does not contain PS1.

Two rounds of behavioral testing were conducted on the mice. The first occurred immediately following repeated mTBIs when the mice were nine weeks old; this allowed us to see short-term effects. The second round took place once the mice reached three months of age, allowing us to examine long-term effects. The mice were aged to eight months before IHC was conducted. This allowed for the brains to mature, along with the possibility of Aβ plaques and tau tangles forming. It was hypothesized that the AD mice

would perform worse on the "daily-living" behavioral tasks (burrowing and nesting) than the WT mice and that the TBI mice would perform worse than the sham mice. To break it down further, it was hypothesized that the AD TBI mice would score the lowest, followed by the AD sham, WT TBI, and WT sham mice, respectively. With immunohistochemistry at 8 months of age, it was hypothesized that the AD mice would show higher levels of APP and GFAP than the WT groups, with TBI being higher than sham. It has previously been found that WT mice do not show Aβ or tau (Tran et al, 2011). With this in mind, only the AD groups were examined for differences in $A\beta_{40}$, $A\beta_{42}$, phospho tau, and total tau. It was also hypothesized the AD mice that received TBI would show higher levels of some or all of the proteins when compared to AD sham.

Behavior

Mice were split into four groups: AD TBI (N = 12), AD sham (N = 13), WT TBI (N = 16), and WT sham (N = 14). The first round of behavioral testing began when the mice were 9 weeks old. As expected, the AD mice performed significantly worse than the WT mice by burrowing less (Table 1 & Figure 1). However, there was no significant difference found between mice that received rmTBI and those that did not. When looking at the 2 hour and 12 hour time points, it is interesting to see that the AD mice burrowed about as much at 12 hours as the WT mice burrowed at 2 hours. This could suggest that AD mice just take longer to perform the task. It would be interesting to see how much the AD mice burrowed at 24 hours and if it would be similar to the WT mice at 12 hours. Similar results were found in the nesting task as in burrowing since AD mice built significantly worse nests than WT mice and no significant difference was found in

relation to TBI (Table 2 & Figure 2). These results agree with a previous study conducted in our lab that found no significant difference between WT mice that received TBI and those that did not on both the burrowing and nesting tasks (Kochen, 2019). (However, the conditions of that experiment were slightly different in that some of the mice were placed under stressful conditions and some were treated with zinc.) In our experiment, a second round of behavioral testing occurred once the mice reached 3 months of age. The only significant difference found for both burrowing and nesting was between genotypes. AD mice burrowed significantly far less than WT mice (Table 3 & Figure 3). However, the WT groups burrowed slightly more than they did in round 1. This could indicate that they learned from the first time which is why they performed better. The AD mice burrowed about the same amount in both rounds showing that they did not learn, or possibly did not remember having done the task already. The AD groups also built significantly worse nests than the WT (Table 4 & Figure 4). Once again, TBI did not have a significant effect on the "daily living" activities.

Other portions of this study were completed by a PhD student (K. Craven) and an undergraduate OSCAR student (T. Gervase). Significant genotype effects were found in all of the other behavioral tasks: open field, elevated zero, Morris water maze, and CR. The behaviors that had a significant interaction effect with TBI were head dips in the elevated zero maze (Craven, 2019) and activity during CR (Gervase, 2019). In CR, AD TBI mice showed a significant increase in activity compared to AD sham, and WT TBI mice showed similar activity to AD sham mice (Gervase, 2019). These significant CR differences appeared during the second round of testing but not the first, suggesting a

delay effect. This suggests that over time the damage to the brain caused by the injuries compound and had a long-term effect on the brain. It was surprising that TBI had no effects on any of the other behavioral tasks. rmTBIs can have long-term effects, so it is possible that behavior was examined too early to see these changes, especially in WT mice.

Immunohistochemistry

To further examine the effect of TBI on AD, IHC was also conducted. Although no behavioral differences due to TBI were seen in this study, CR differences due to TBI were seen by Gervase (2019). Thus, it is possible that there is a difference in brain pathology for AD mice and TBI mice compared to WT sham, since damage to the brain often begins ten years or more before behavioral symptoms in humans (Alzheimer's Disease Education and Referral Center, 2016). Previous research has found that TBI causes APP to accumulate, followed by Aβ production (Blennow, Hardy, & Zetterberg, 2012). An increase in hyperphosphorylated tau using IHC has also been found following TBI (Sivanandam & Thakur, 2012). A majority of these findings came from elderly mice, between 8 and 15 months of age. IHC was used to visualize the location of important proteins associated with AD and TBI in this study. The tau tangles produced from TBI are similar to those found in AD patients but in somewhat different locations (Blennow, Hardy, & Zetterberg, 2012). An increase of APP accumulation is also seen following TBI which leads to the production of Aβ (Blennow, Hardy, & Zetterberg, 2012). These plaques from TBI are thus comparable to AD plaque formation. These data suggest that when AD and TBI are combined, they could cause an increase in either or both Aβ and

phospho tau. To test this, we examined APP, $A\beta_{40}$, $A\beta_{42}$, phospho tau, and total tau using IHC. GFAP was also included to measure possible inflammation caused by the injuries. The brain regions of focus were the hippocampus and infralimbic cortex, as both play a large role in AD.

APP and GFAP

APP and GFAP were analyzed in all four groups. As expected, mice with AD displayed higher APP levels (measured through percent area) in the HC than WT mice (Table 5, Figures 5 & 6). AD TBI mice showed higher levels of APP in the HC followed by AD sham, WT sham, and WT TBI, respectively. It is likely that the axonal damaged caused by the injuries led to the accumulation of APP. However, there was no difference in APP levels at the IL. This could mean that the APP proteins migrated to the HC, or that there were more located in the HC to begin with and the TBIs built on what was already there due to AD. GFAP was also higher in AD mice compared to WT (Table 5 & 7, Figures 5, 6, 9, & 10). TBI mice did not show higher levels of GFAP as expected, although it is often connected to brain injuries. An increase in GFAP levels has often been noted to occur immediately after TBI. It is possible that in this experiment levels may have decreased over time, as levels were not examined until the mice were 8 months old. If GFAP had been measured directly following the TBIs, it is more likely a difference would have been found.

Phospho Tau and Total Tau

Phospho tau and total tau were only examined within the AD groups since previous work has shown no difference in WT (Tran et al, 2011). Higher phospho tau

levels were found in the HC of the AD TBI mice (Table 6, Figures 7 & 8). This adds to previous research having found that TBI increased hyperphosphoralated tau (Iliff et al, 2014). However, there was no difference in total tau levels between AD TBI and AD sham. These results suggest that TBI affects the state of phosphorylation of tau and not the amount of tau present or produced. This adds to the research supporting TBI increasing tau phosphoralation. A similar lack of significant difference in pathology was found in the IL for total tau and also phospho tau. However, the pattern seen with both phospho tau and total tau within the HC are similar to those found in the IL. The lack of significance in the IL could be due to the large SDs. This increase in phospho tau for the AD TBI mice aligns with the findings from the western blots (Craven, 2019). Higher levels of phospho tau were noted in the AD TBI brains compared to the AD sham brains. These findings support the dual pathway hypothesis which states that Aβ plaques and tau tangles form simultaneously, as opposed to the amyloid hypothesis that says Aβ leads to the hyperphosphorylation of tau.

$A\beta_{40}$ and $A\beta_{42}$

$A\beta_{40}$ and $A\beta_{42}$ were also only compared between the AD groups. When $A\beta_{40}$ and $A\beta_{42}$ were examined between the AD TBI mice and the AD sham mice, no difference in levels were found (Tables 7 & 8, Figures 7, 8, 11, & 12). Although there were no significant differences in $A\beta_{40}$ and $A\beta_{42}$, $A\beta_{40}$ appeared higher than $A\beta_{42}$ in the HC. It is unclear why this occurred, but it is thought is that a majority of secreted Aβ is in the form $A\beta_{40}$. It is thought that $A\beta_{40}$ inhibits $A\beta_{42}$ plaque formation (Zou et al, 2013). This could account for why there was less $A\beta_{42}$ in the HC when there were higher levels of $A\beta_{40}$.

However, $A\beta_{42}$ did show a strong trend in the IL for the AD TBI mice ($p = 0.062$) and when a Mann Whitney U-test was run, a significant difference was found ($p = 0.029$) (Table 8, Figures 11 & 12).

Other Results

Another aspect of this study included the thioflavin-s stain to visualize tangles and the congo red stain to visualize plaques. When examining tangle formation through the use of the thioflavin-s stain, the infralimbic cortex showed a significantly higher number of tangles following TBI (Craven, 2019). However, thioflavin-s is not as specific as IHC because it tags β-pleated sheets, which includes tau tangles and Aβ plaques. The two proteins will look different, which is how they can be distinguished, but this could be subjective. IHC specifically tags phospho tau, whereas theoflavin-s stains β-pleated sheets and the interpretation relies on morphology. This makes it difficult to directly compare the results. IHC within the infralimbic cortex showed AD mice to have a higher percent areas of both APP and GFAP than the WT mice (Table 7, Figures 9 & 10). No difference was found due to TBI. There was also no statistically significant difference shown by the congo red stain, although AD TBI mice showed, on average, more Aβ plaques in the HC than AD sham mice (Craven, 2019).

Summary

The IHC results show the pathology presence found in the AD brains was as expected. Our results also showed an increase in APP and phospho tau localized in the hippocampus of AD mice that received TBI. This increase supports previous research indicating that TBI causes an increase in APP and the hyperphosphoralation of tau when

paired with AD. However, we did not see an increase in any other pathologies associated with TBI, although there was a pattern of higher means and large SDs. These may in part be due to the strong effect AD has on brain pathology which could overpower the effects of TBI. A larger sample size could decrease the variation and allow for a better analysis of the antibodies. This could also be accomplished by analyzing more than one slice per antibody per brain. An average of each antibody for each brain would allow for a better representation. See Tables 9 and 10 for overall effects summary.

These results also show the difference between our AD mice and WT mice in behavior and IHC. This helps to support our novel APP/tau mouse model as being similar to AD human patients. The results show that our AD mice show behavioral deficits consistent with those seen in humans. Patients with AD show a decrease in the ability to complete simple daily-living activities such as getting dressed in the morning. When tested for "daily-living" activities through the burrowing and nesting tasks, our AD mice also showed the inability to complete these instinctual activities.

Table 9. Immunohistochemistry summary of the hippocampus. A brief summary for APP, $A\beta_{40}$, $A\beta_{42}$, phospho tau, total tau, and GFAP in the HC.

APP	Significant genotype effect (AD higher than WT) Significant interaction (AD TBI highest)
$A\beta_{40}$	No significance, but high SDs (AD TBI higher than AD sham)
$A\beta_{42}$	No significance, very low values
Phospho Tau	Significant TBI effect (AD TBI higher than AD sham)
Total Tau	No significance, similar pattern to IL (AD TBI higher than AD sham)
GFAP	Significant genotype effect (AD higher than WT) No significant interaction (AD sham slightly higher)

Table 10. Immunohistochemistry summary of the infralimbic cortex. A brief summary for APP, $A\beta_{40}$, $A\beta_{42}$, phospho tau, total tau, and GFAP in the HC.

APP	Significant genotype effect (AD higher than WT) No significant interaction (AD TBI slightly higher)
$A\beta_{40}$	No significance, but high SDs (AD TBI higher than AD sham)
$A\beta_{42}$	No significance but trending (AD TBI higher than AD sham)
Phospho Tau	No significance (AD TBI higher than AD sham)
Total Tau	No significance, similar pattern to HC (AD TBI higher than AD sham)
GFAP	Significant genotype effect (AD higher than WT) No significant interaction (AD TBI slightly higher)

Although APP, GFAP, and $A\beta_{42}$ showed a significant difference in protein amount between the HC and IL (with the HC being higher), $A\beta_{40}$, phospho tau, and total tau did not. AD brains often display higher levels of these proteins in the HC while TBI patients see these proteins spread throughout the brain, including the IL. Throughout the study, AD TBI brains continued to show higher levels of each protein in both the HC and IL compared to the AD shams. This pattern suggests that TBI is affacting the brain although the findings are not significant.

To further this research, it would be interesting to examine levels of Aβ, tau, and GFAP at different time periods. We waited until 8 months to examine the brains. This allowed for the production of Aβ plaques and tau tangles to form due to the AD mutations. This happens over a longer period of time, whereas following TBI Aβ appears much sooner. It is possible that Aβ levels are higher early-on in AD mice having received TBI than those that did not. In this case, Aβ would be different in TBI vs sham AD mice

at an earlier time point but production would catch up in the shams over time. Earlier analysis could help create a timeline on the pathology formation.

These experiments showed changes in APP of both AD and WT mice and phospho tau of AD mice due to TBI. Similar patterns were seen amongst the other antibodies ($A\beta_{40}$, $A\beta_{42}$, total tau, and GFAP) but they displayed higher SDs and where therefor not significant. IHC was conducted on 8 month brains, once AD pathologies were well established. This emphasizes a continued need for more data collection due to the persisting occurrence of TBIs in the population and the need to further understand the causes of AD.

APPENDIX

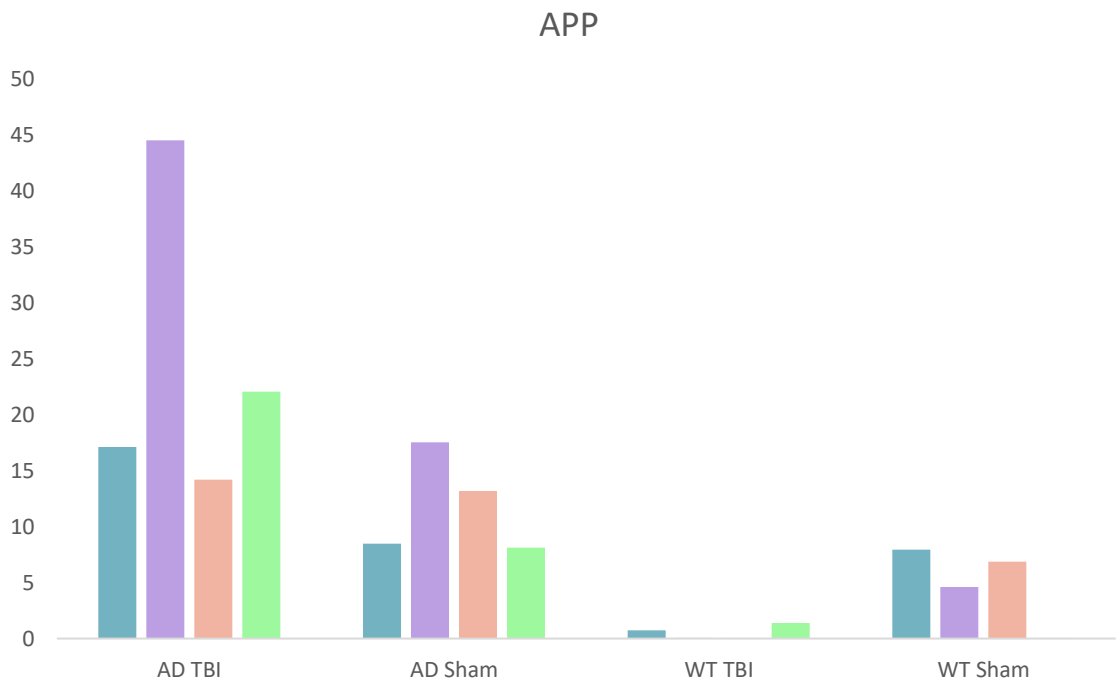

Figure 13. Individual APP immunohistochemistry scores of the hippocampus. Percent area of protein present within the hippocampus normalized to the correct isotype control (as described in methods) for APP of each brain within the four groups.

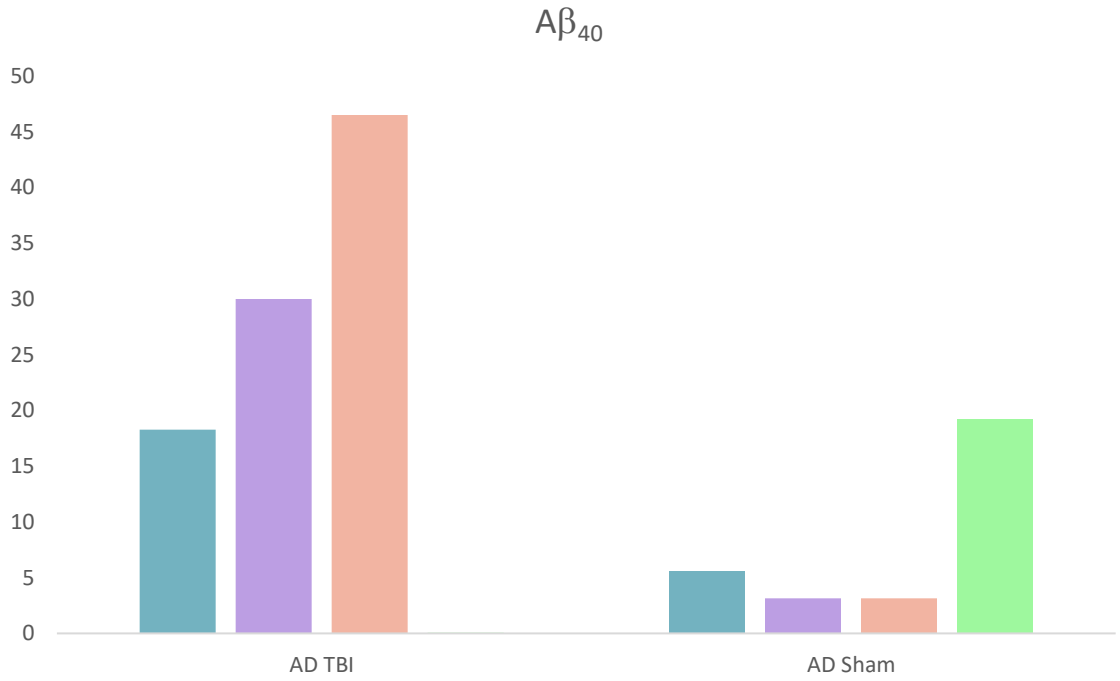

Figure 14. Individual Aβ40 immunohistochemistry scores of the hippocampus. Percent area of protein present within the hippocampus normalized to the correct isotype control (as described in methods) for Aβ40 of each brain within the AD groups.

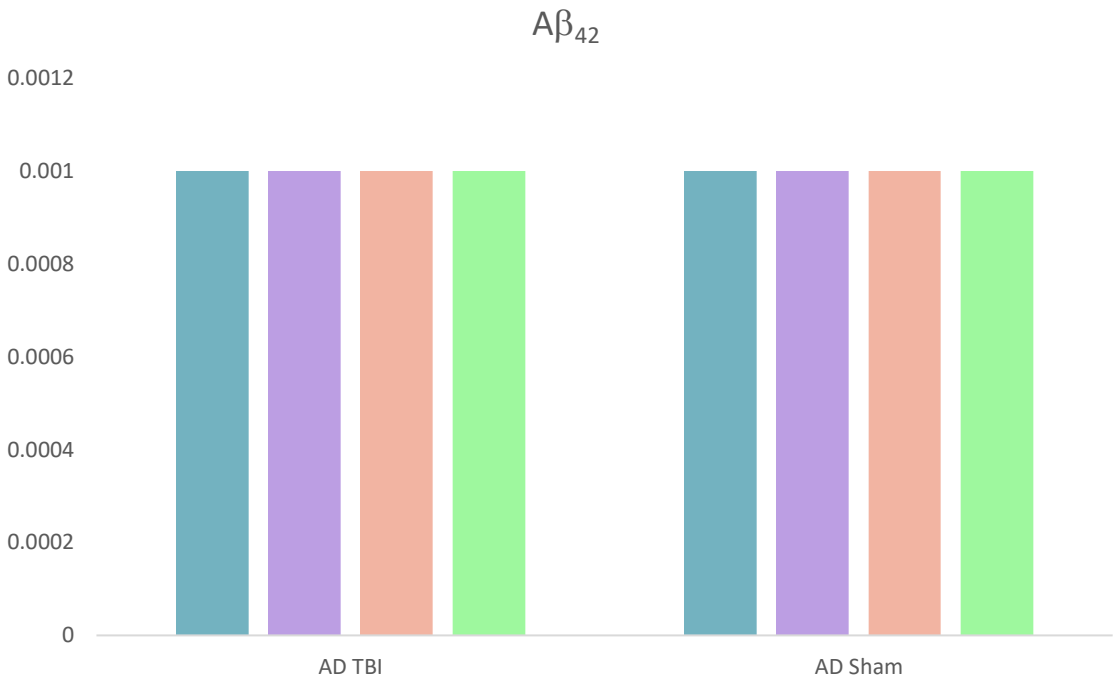

Figure 15. Individual Aβ42 immunohistochemistry scores of the hippocampus. Percent area of protein present within the hippocampus normalized to the correct isotype control (as described in methods) for Aβ42 of each brain within the AD groups.

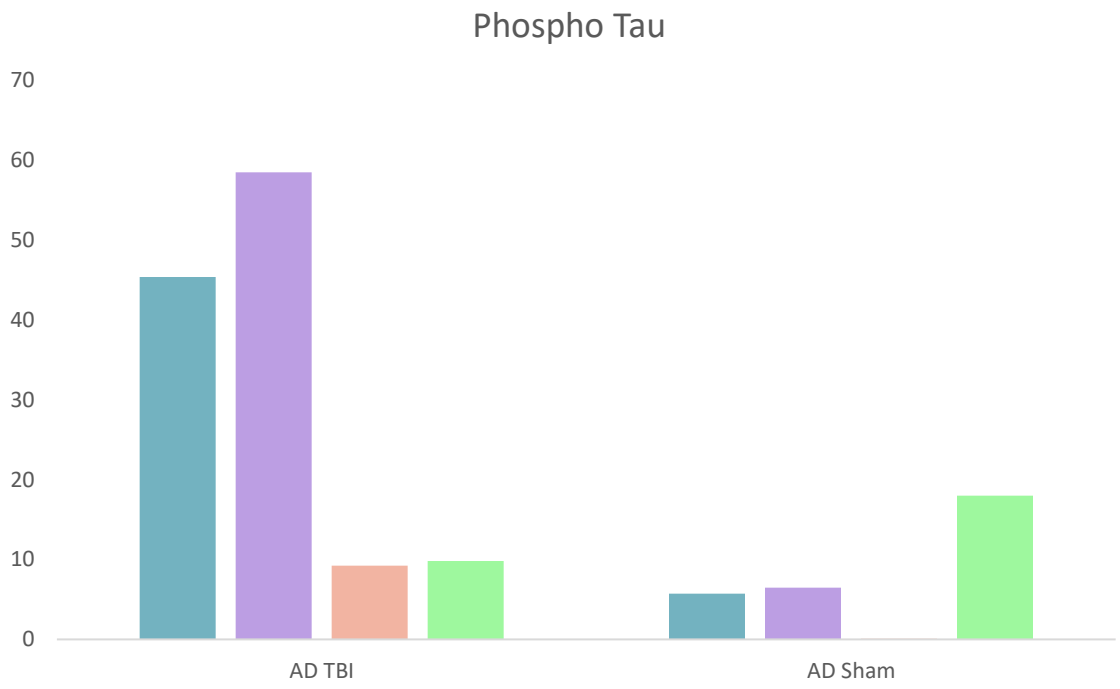

Figure 16. Individual phospho tau immunohistochemistry scores of the hippocampus. Percent area of protein present within the hippocampus normalized to the correct isotype control (as described in methods) for phospho tau of each brain within the AD groups.

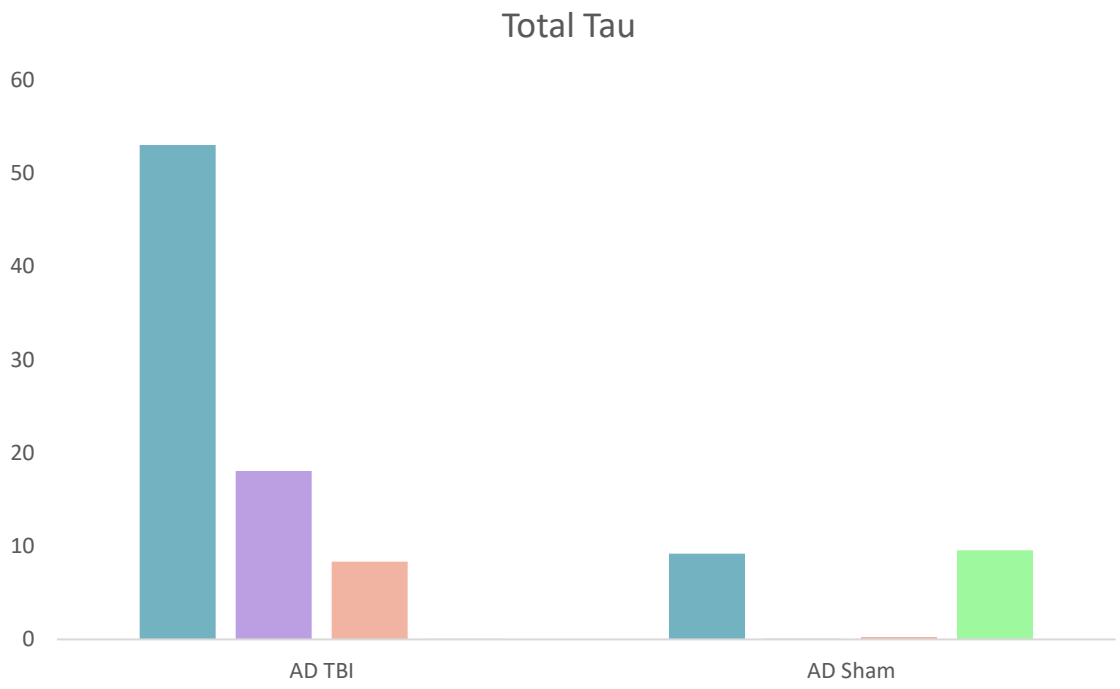

Figure 17. Individual total tau immunohistochemistry scores of the hippocampus. Percent area of protein present within the hippocampus normalized to the correct isotype control (as described in methods) for total tau of each brain within the AD groups.

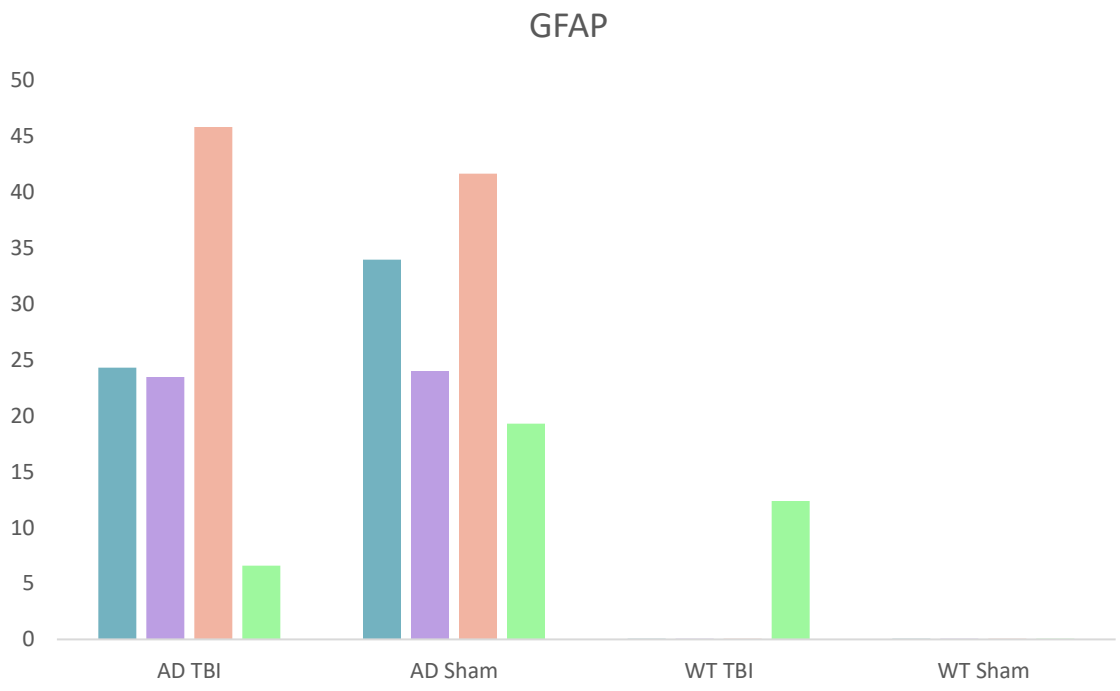

Figure 18. Individual GFAP immunohistochemistry scores of the hippocampus. Percent area of protein present within the hippocampus normalized to the correct isotype control (as described in methods) for GFAP of each brain within the four groups.

Figure 19. Individual APP immunohistochemistry scores of the infralimbic cortex. Percent area of protein present within the infralimbic cortex normalized to the correct isotype control (as described in methods) for APP of each brain within the four groups.

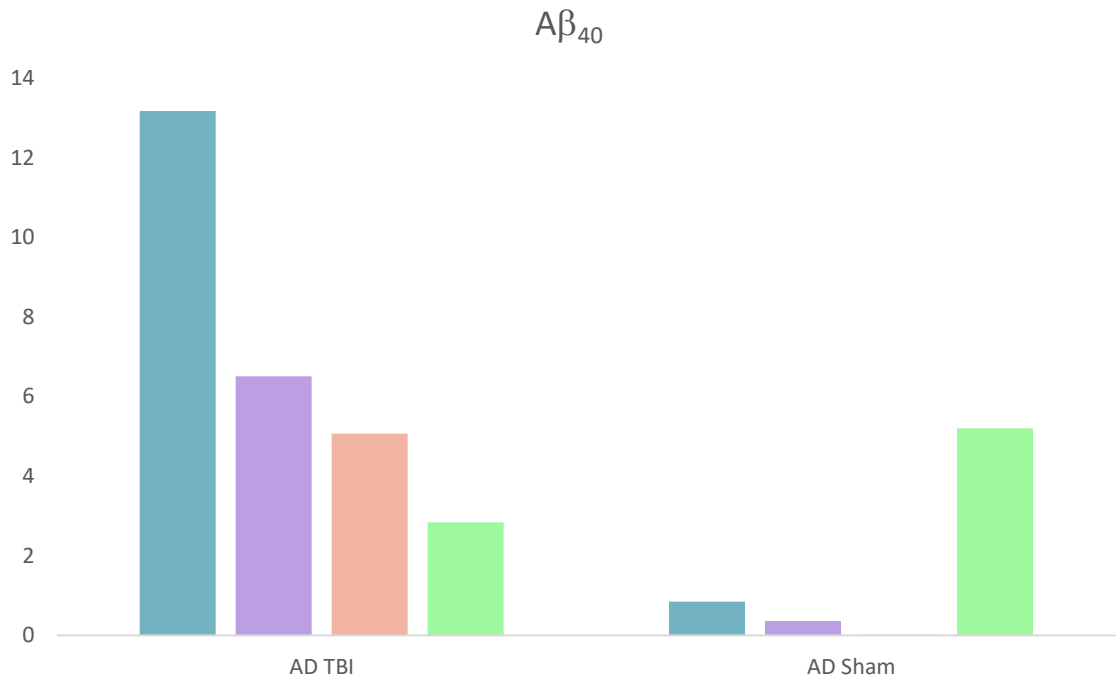

Figure 20. Individual Aβ40 immunohistochemistry scores of the infralimbic cortex. Percent area of protein present within the infralimbic cortex normalized to the correct isotype control (as described in methods) for Aβ40 of each brain within the AD groups.

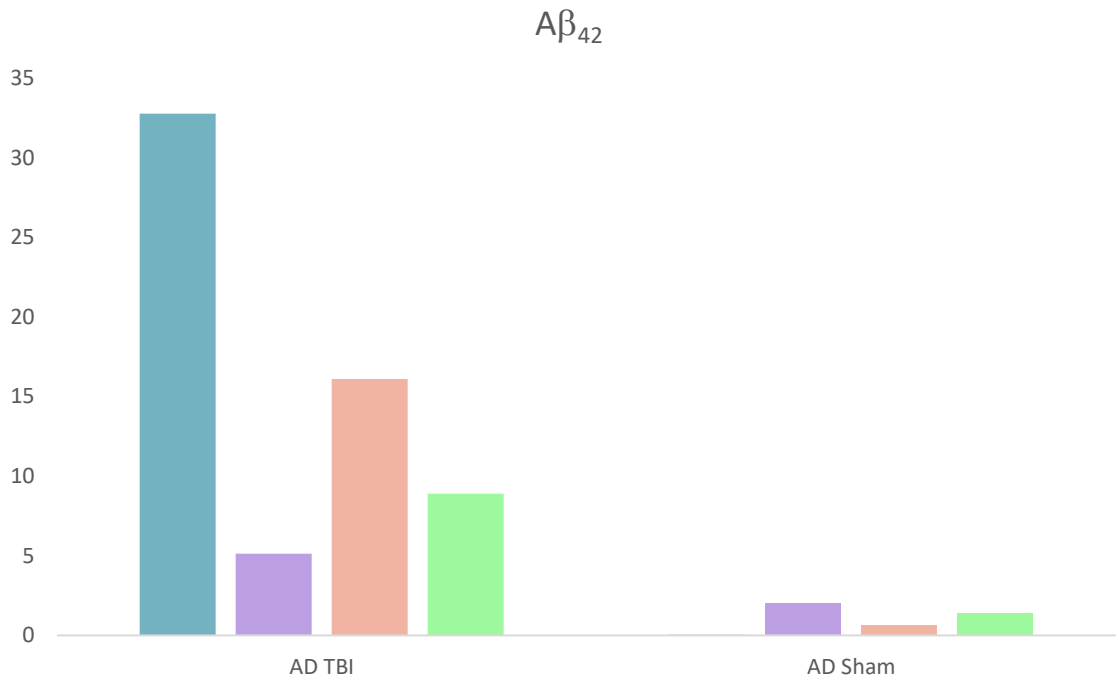

Figure 21. Individual Aβ42 immunohistochemistry scores of the infralimbic cortex. Percent area of protein present within the infralimbic cortex normalized to the correct isotype control (as described in methods) for Aβ42 of each brain within the AD groups.

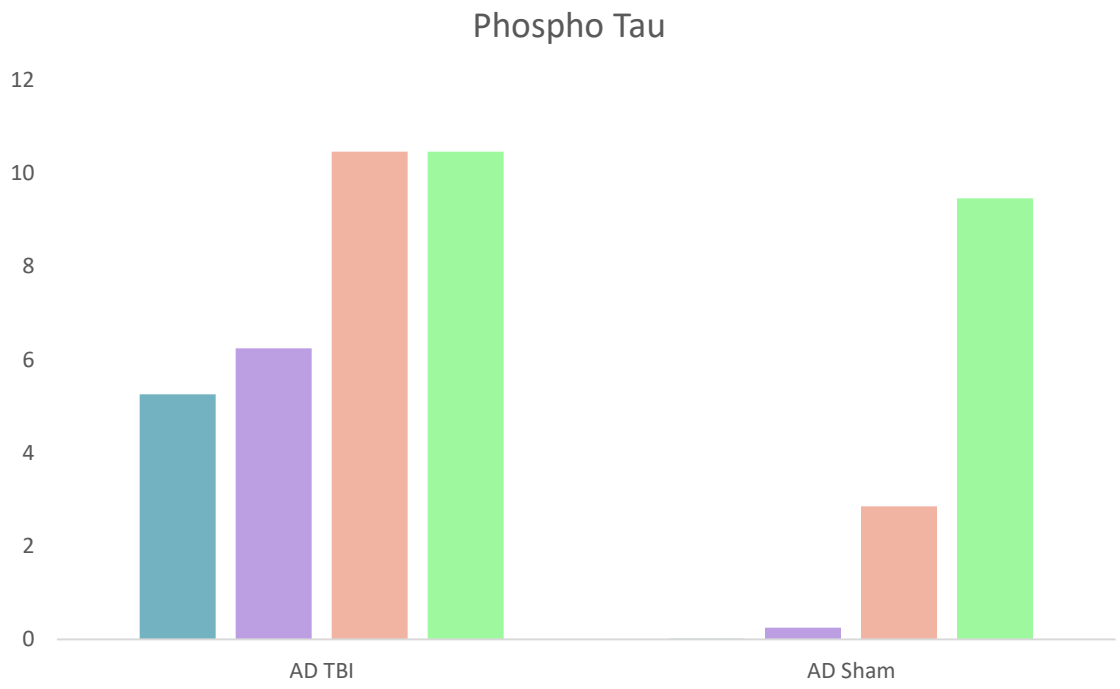

Figure 22. Individual phospho tau immunohistochemistry scores of the infralimbic cortex. Percent area of protein present within the infralimbic cortex normalized to the correct isotype control (as described in methods) for phospho tau of each brain within the AD groups.

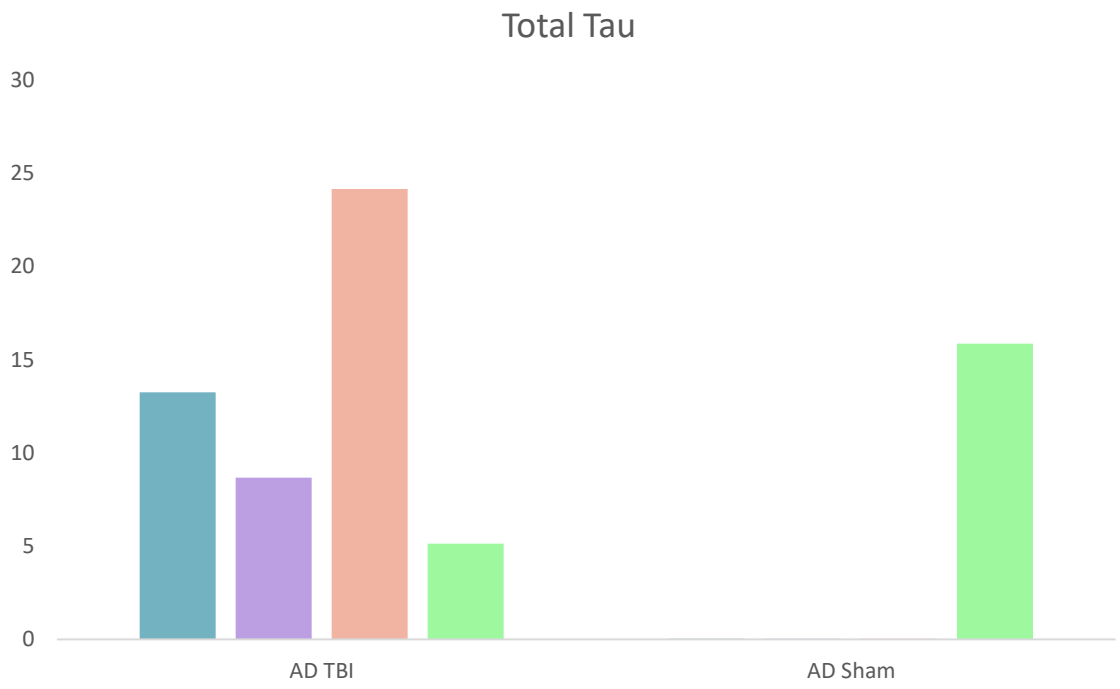

Figure 23. Individual total tau immunohistochemistry scores of the infralimbic cortex. Percent area of protein present within the infralimbic cortex normalized to the correct isotype control (as described in methods) for total tau of each brain within the AD groups.

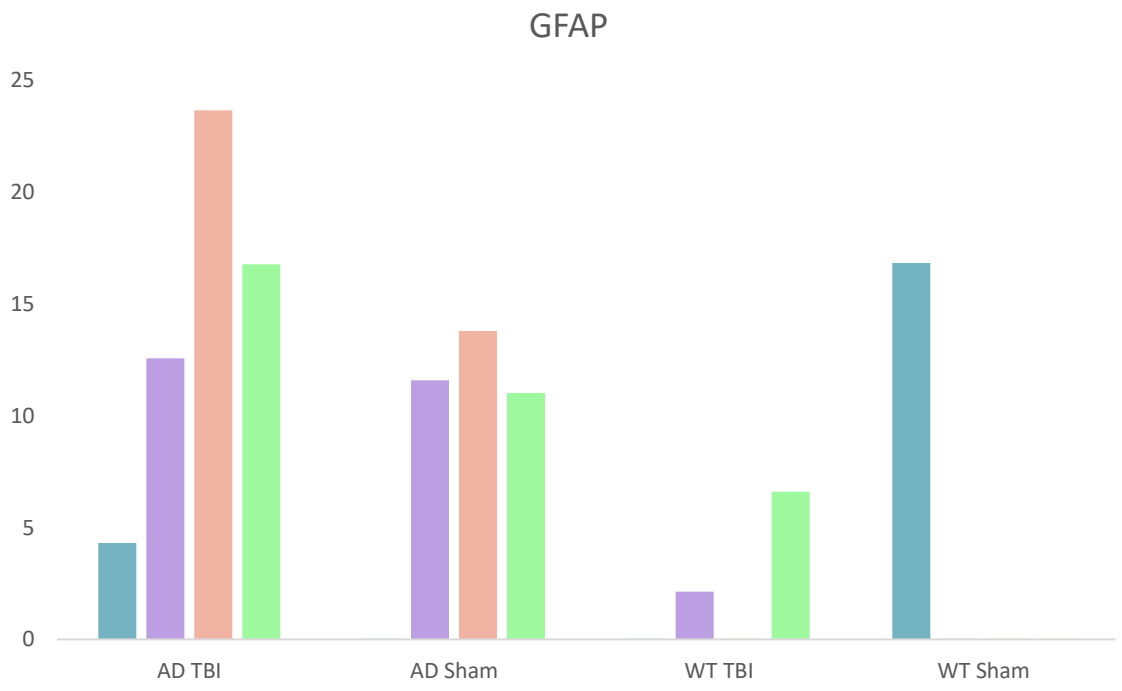

Figure 24. Figure 19. Individual GFAP immunohistochemistry scores of the infralimbic cortex. Percent area of protein present within the infralimbic cortex normalized to the correct isotype control (as described in methods) for GFAP of each brain within the four groups.

Table 11. Individual immunohistochemistry scores of the hippocampus for AD TBI. Measured percent area of protein present within the hippocampus. Data were normalized to the correct isotype control (as described in methods) for each brain within the antibodies: APP, $A\beta_{40}$, $A\beta_{42}$, phospho tau, total tau, and GFAP.

Antibody	Percent Area	Normalized
0.1 µl/ml Rabbit Polyclonal Isotype Control APP	9.374	
0.1 µl/ml APP	26.506	17.132
0.1 µl/ml APP	53.945	44.571
0.1 µl/ml APP	23.563	14.189
0.1 µl/ml APP	31.445	22.071
0.0005 µl/ml Rabbit Polyclonal Isotype Control $A\beta_{40}$	21.176	

0.0005 µl/ml $A\beta_{40}$	39.472	18.296
0.0005 µl/ml $A\beta_{40}$	51.2	30.024
0.0005 µl/ml $A\beta_{40}$	67.692	46.516
0.0005 µl/ml $A\beta_{40}$	9.405	-11.771
0.00167 µl/ml Rabbit Polyclonal Isotype Control $A\beta_{42}$	14.726	
0.00167 µl/ml $A\beta_{42}$	7.524	-7.202
0.00167 µl/ml $A\beta_{42}$	5.907	-8.819
0.00167 µl/ml $A\beta_{42}$	12.786	-1.94
0.00167 µl/ml $A\beta_{42}$	7.386	-7.34
0.0000455 µl/ml Rabbit Monoclonal Isotype Control Phospho Tau	5.752	
0.0000455 µl/ml Phospho Tau	51.085	45.333
0.0000455 µl/ml Phospho Tau	64.214	58.462
0.0000455 µl/ml Phospho Tau	15.013	9.261
0.0000455 µl/ml Phospho Tau	15.543	9.791
0.0001 µl/ml Mouse Monoclonal Isotype Control Total Tau	8.867	
0.0001 µl/ml Total Tau	61.939	53.072
0.0001 µl/ml Total Tau	26.943	18.076
0.0001 µl/ml Total Tau	17.239	8.372
0.0001 µl/ml Total Tau	7.333	-1.534
0.00004 µl/ml Mouse Monoclonal Isotype Control GFAP	9.365	
0.00004 µl/ml GFAP	33.662	24.297
0.00004 µl/ml GFAP	32.81	23.445
0.00004 µl/ml GFAP	55.155	45.79
0.00004 µl/ml GFAP	15.93	6.565

Table 12. Individual immunohistochemistry scores of the hippocampus for AD sham. Measured percent area of protein present within the hippocampus. Data were normalized to the correct isotype control (as described in methods) for each brain within the antibodies: APP, $A\beta_{40}$, $A\beta_{42}$, phospho tau, total tau, and GFAP.

Antibody	Percent Area	Normalized
0.1 µl/ml Rabbit Polyclonal Isotype Control APP	7.65	
0.1 µl/ml APP	16.157	8.507
0.1 µl/ml APP	25.169	17.519
0.1 µl/ml APP	20.824	13.174
0.1 µl/ml APP	15.753	8.103
0.0005 µl/ml Rabbit Polyclonal Isotype Control $A\beta_{40}$	8.535	
0.0005 µl/ml $A\beta_{40}$	14.152	5.617
0.0005 µl/ml $A\beta_{40}$	11.677	3.142
0.0005 µl/ml $A\beta_{40}$	11.664	3.129
0.0005 µl/ml $A\beta_{40}$	27.789	19.254
0.00167 µl/ml Rabbit Polyclonal Isotype Control $A\beta_{42}$	9.879	
0.00167 µl/ml $A\beta_{42}$	5.906	-3.973
0.00167 µl/ml $A\beta_{42}$	8.822	-1.057
0.00167 µl/ml $A\beta_{42}$	8.032	-1.847
0.00167 µl/ml $A\beta_{42}$	6.923	-2.956
0.0000455 µl/ml Rabbit Monoclonal Isotype Control Phospho Tau	17.674	
0.0000455 µl/ml Phospho Tau	23.374	5.7
0.0000455 µl/ml Phospho Tau	24.135	6.461
0.0000455 µl/ml Phospho Tau	16.267	-1.407
0.0000455 µl/ml Phospho Tau	35.669	17.995
0.0001 µl/ml Mouse Monoclonal Isotype Control Total Tau	17.062	

0.0001 µl/ml Total Tau	26.23	9.168
0.0001 µl/ml Total Tau	5.388	-11.674
0.0001 µl/ml Total Tau	17.334	0.272
0.0001 µl/ml Total Tau	26.651	9.589
0.00004 µl/ml Mouse Monoclonal Isotype Control GFAP	4.221	
0.00004 µl/ml GFAP	38.164	33.943
0.00004 µl/ml GFAP	28.208	23.987
0.00004 µl/ml GFAP	45.868	41.647
0.00004 µl/ml GFAP	23.508	19.287

Table 13. Individual immunohistochemistry scores of the hippocampus for WT TBI. Measured percent area of protein present within the hippocampus. Data were normalized to the correct isotype control (as described in methods) for each brain within the antibodies: APP, $A\beta_{40}$, $A\beta_{42}$, phospho tau, total tau, and GFAP.

Antibody	Percent Area	Normalized
0.1 µl/ml Rabbit Polyclonal Isotype Control APP	10.415	
0.1 µl/ml APP	11.174	0.759
0.1 µl/ml APP	8.383	-2.032
0.1 µl/ml APP	7.541	-2.874
0.1 µl/ml APP	11.821	1.406
0.0005 µl/ml Rabbit Polyclonal Isotype Control $A\beta_{40}$	16.841	
0.0005 µl/ml $A\beta_{40}$	12.085	-4.756
0.00167 µl/ml Rabbit Polyclonal Isotype Control $A\beta_{42}$	2.808	
0.00167 µl/ml $A\beta_{42}$	8.345	5.537
0.0000455 µl/ml Rabbit Monoclonal Isotype Control Phospho Tau	3.363	
0.0000455 µl/ml Phospho Tau	14	10.637

0.0001 µl/ml Mouse Monoclonal Isotype Control Total Tau	12.164	
0.0001 µl/ml Total Tau	21.579	9.415
0.00004 µl/ml Mouse Monoclonal Isotype Control GFAP	11.239	
0.00004 µl/ml GFAP	2.814	-8.425
0.00004 µl/ml GFAP	2.082	-9.157
0.00004 µl/ml GFAP	3.726	-7.513
0.00004 µl/ml GFAP	23.638	12.399

Table 14. Individual immunohistochemistry scores of the hippocampus for WT sham. Measured percent area of protein present within the hippocampus. Data were normalized to the correct isotype control (as described in methods) for each brain within the antibodies: APP, $A\beta_{40}$, $A\beta_{42}$, phospho tau, total tau, and GFAP.

Antibody	Percent Area	Normalized
0.1 µl/ml Rabbit Polyclonal Isotype Control APP	7.277	
0.1 µl/ml APP	15.222	7.945
0.1 µl/ml APP	11.91	4.633
0.1 µl/ml APP	14.161	6.884
0.1 µl/ml APP	1.601	-5.676
0.0005 µl/ml Rabbit Polyclonal Isotype Control $A\beta_{40}$	7.361	
0.0005 µl/ml $A\beta_{40}$	19.071	11.71
0.00167 µl/ml Rabbit Polyclonal Isotype Control $A\beta_{42}$	30.875	
0.00167 µl/ml $A\beta_{42}$	36.617	5.742
0.0000455 µl/ml Rabbit Monoclonal Isotype Control Phospho Tau	5.132	
0.0000455 µl/ml Phospho Tau	11.714	6.582

0.0001 µl/ml Mouse Monoclonal Isotype Control Total Tau	11.522	
0.0001 µl/ml Total Tau	20.979	9.457
0.00004 µl/ml Mouse Monoclonal Isotype Control GFAP	15.336	
0.00004 µl/ml GFAP	5.487	-9.849
0.00004 µl/ml GFAP	5.823	-9.513
0.00004 µl/ml GFAP	8.767	-6.569
0.00004 µl/ml GFAP	13.054	-2.282

Table 15. Individual immunohistochemistry scores of the infralimbic cortex for AD TBI. Measured percent area of protein present within the infralimbic cortex. Data were normalized to the correct isotype control (as described in methods) for each brain within the antibodies: APP, $A\beta_{40}$, $A\beta_{42}$, phospho tau, total tau, and GFAP.

Antibody	Percent Area	Normalized
0.1 µl/ml Rabbit Polyclonal Isotype Control APP	11.288	
0.1 µl/ml APP	18.822	7.534
0.1 µl/ml APP	12.776	1.488
0.1 µl/ml APP	14.822	3.534
0.1 µl/ml APP	13.434	2.146
0.0005 µl/ml Rabbit Polyclonal Isotype Control $A\beta_{40}$	9.001	
0.0005 µl/ml $A\beta_{40}$	22.169	13.168
0.0005 µl/ml $A\beta_{40}$	15.514	6.513
0.0005 µl/ml $A\beta_{40}$	14.076	5.075
0.0005 µl/ml $A\beta_{40}$	11.836	2.835
0.00167 µl/ml Rabbit Polyclonal Isotype Control $A\beta_{42}$	7.076	
0.00167 µl/ml $A\beta_{42}$	39.833	32.757
0.00167 µl/ml $A\beta_{42}$	12.209	5.133
0.00167 µl/ml $A\beta_{42}$	23.168	16.092
0.00167 µl/ml $A\beta_{42}$	15.975	8.899

0.0000455 µl/ml Rabbit Monoclonal Isotype Control Phospho Tau	2.469	
0.0000455 µl/ml Phospho Tau	7.729	5.26
0.0000455 µl/ml Phospho Tau	8.716	6.247
0.0000455 µl/ml Phospho Tau	12.931	10.462
0.0000455 µl/ml Phospho Tau	12.935	10.466
0.0001 µl/ml Mouse Monoclonal Isotype Control Total Tau	9.041	
0.0001 µl/ml Total Tau	22.296	13.255
0.0001 µl/ml Total Tau	17.729	8.688
0.0001 µl/ml Total Tau	33.216	24.175
0.0001 µl/ml Total Tau	14.17	5.129
0.00004 µl/ml Mouse Monoclonal Isotype Control GFAP	12.397	
0.00004 µl/ml GFAP	16.698	4.301
0.00004 µl/ml GFAP	24.962	12.565
0.00004 µl/ml GFAP	36.054	23.657
0.00004 µl/ml GFAP	29.157	16.76

Table 16. Individual immunohistochemistry scores of the infralimbic cortex for AD sham. Measured percent area of protein present within the infralimbic cortex. Data were normalized to the correct isotype control (as described in methods) for each brain within the antibodies: APP, $A\beta_{40}$, $A\beta_{42}$, phospho tau, total tau, and GFAP.

Antibody	Percent Area	Normalized
0.1 µl/ml Rabbit Polyclonal Isotype Control APP	10.756	
0.1 µl/ml APP	9.785	-0.971
0.1 µl/ml APP	9.8	-0.956
0.1 µl/ml APP	5.763	-4.993
0.1 µl/ml APP	18.112	7.356

0.0005 µl/ml Rabbit Polyclonal Isotype Control $A\beta_{40}$	9.326	
0.0005 µl/ml $A\beta_{40}$	10.18	0.854
0.0005 µl/ml $A\beta_{40}$	9.683	0.357
0.0005 µl/ml $A\beta_{40}$	8.644	-0.682
0.0005 µl/ml $A\beta_{40}$	14.522	5.196
0.00167 µl/ml Rabbit Polyclonal Isotype Control $A\beta_{42}$	10.5	
0.00167 µl/ml $A\beta_{42}$	8.874	-1.626
0.00167 µl/ml $A\beta_{42}$	12.555	2.055
0.00167 µl/ml $A\beta_{42}$	11.154	0.654
0.00167 µl/ml $A\beta_{42}$	11.919	1.419
0.0000455 µl/ml Rabbit Monoclonal Isotype Control Phospho Tau	13.534	
0.0000455 µl/ml Phospho Tau	5.584	-7.95
0.0000455 µl/ml Phospho Tau	13.783	0.249
0.0000455 µl/ml Phospho Tau	16.391	2.857
0.0000455 µl/ml Phospho Tau	22.999	9.465
0.0001 µl/ml Mouse Monoclonal Isotype Control Total Tau	9.175	
0.0001 µl/ml Total Tau	8.226	-0.949
0.0001 µl/ml Total Tau	8.847	-0.328
0.0001 µl/ml Total Tau	7.268	-1.907
0.0001 µl/ml Total Tau	25.046	15.871
0.00004 µl/ml Mouse Monoclonal Isotype Control GFAP	8.262	
0.00004 µl/ml GFAP	6.87	-1.392
0.00004 µl/ml GFAP	19.853	11.591
0.00004 µl/ml GFAP	22.05	13.788
0.00004 µl/ml GFAP	19.288	11.026

Table 17. Individual immunohistochemistry scores of the infralimbic cortex for WT TBI. Measured percent area of protein present within the infralimbic cortex. Data were normalized to the correct isotype control (as described in methods) for each brain within the antibodies: APP, $A\beta_{40}$, $A\beta_{42}$, phospho tau, total tau, and GFAP.

Antibody	Percent Area	Normalized
0.1 µl/ml Rabbit Polyclonal Isotype Control APP	28.159	
0.1 µl/ml APP	4.352	-23.807
0.1 µl/ml APP	6.181	-21.978
0.1 µl/ml APP	3.26	-24.899
0.1 µl/ml APP	6.657	-21.502
0.0005 µl/ml Rabbit Polyclonal Isotype Control $A\beta_{40}$	27.317	
0.0005 µl/ml $A\beta_{40}$	26.646	-0.671
0.00167 µl/ml Rabbit Polyclonal Isotype Control $A\beta_{42}$	11.566	
0.00167 µl/ml $A\beta_{42}$	6.076	-5.49
0.0000455 µl/ml Rabbit Monoclonal Isotype Control Phospho Tau	6.229	
0.0000455 µl/ml Phospho Tau	20.142	13.913
0.0001 µl/ml Mouse Monoclonal Isotype Control Total Tau	11.001	
0.0001 µl/ml Total Tau	21.798	10.797
0.00004 µl/ml Mouse Monoclonal Isotype Control GFAP	9.628	
0.00004 µl/ml GFAP	5.728	-3.9
0.00004 µl/ml GFAP	11.75	2.122
0.00004 µl/ml GFAP	7.795	-1.833
0.00004 µl/ml GFAP	16.241	6.613

Table 18. Individual immunohistochemistry scores of the infralimbic cortex for WT sham. Measured percent area of protein present within the infralimbic cortex. Data were normalized to the correct isotype control (as described in methods) for each brain within the antibodies: APP, $A\beta_{40}$, $A\beta_{42}$, phospho tau, total tau, and GFAP.

Antibody	Percent Area	Normalized
0.1 µl/ml Rabbit Polyclonal Isotype Control APP	33.376	
0.1 µl/ml APP	5.419	-27.957
0.1 µl/ml APP	5.859	-27.517
0.1 µl/ml APP	5.495	-27.881
0.1 µl/ml APP	5.811	-27.565
0.0005 µl/ml Rabbit Polyclonal Isotype Control $A\beta_{40}$	6.087	
0.0005 µl/ml $A\beta_{40}$	20.181	14.094
0.00167 µl/ml Rabbit Polyclonal Isotype Control $A\beta_{42}$	39.279	
0.00167 µl/ml $A\beta_{42}$	13.188	-26.091
0.0000455 µl/ml Rabbit Monoclonal Isotype Control Phospho Tau	13.445	
0.0000455 µl/ml Phospho Tau	22.927	9.482
0.0001 µl/ml Mouse Monoclonal Isotype Control Total Tau	19.662	
0.0001 µl/ml Total Tau	18.786	-0.876
0.00004 µl/ml Mouse Monoclonal Isotype Control GFAP	16.712	
0.00004 µl/ml GFAP	33.547	16.835
0.00004 µl/ml GFAP	5.594	-11.118
0.00004 µl/ml GFAP	6.009	-10.703
0.00004 µl/ml GFAP	19.883	3.171

REFERENCES

Alzheimer's Association. (2016). Alzheimer's disease facts and figures. *Alzheimer's & Dementia, 12.*

Alzheimer's Disease Education and Referral Center. (2016). Alzheimer's disease: Fact sheet. *National Institute on Aging*.

Bäckman, L., Jones, S., Berger, A. K., Laukka, E. J., Small, B. J. (2004). Multiple cognitive deficits during the transition to Alzheimer's disease. *Journal of Internal Medicine, 256,* 195-204.

Blennow, K., Hardy, J., & Zetterberg, H. (2012). The neuropathology and neurobiology of traumatic brain injury. *Neuron, 76*(5), 886-899.

Braak, H. & Braak, E. (1991). Neuropathological staging of Alzheimer-related changes. *Acta Neuropathologica, 82,* 239-259.

Cheng, W. H., Stukas, S., Martens, K. M., Namjoshi, D. R., Button, E. B., Wilkinson, A., Bashir, A., Robert, J., Cripton, P. A., & Wellington, C. L. (2018). Age at injury and genotype modify acute inflammatory and neurofilament-light responses to mild CHIMERA traumatic brain injury in wild-type and APP/PS1 mice. *Experimental Neurology, 301,* 26-38.

Craven, K. M. (2019). Repetitive mild traumatic brain injury exacerbates the progression of Alzheimer's disease in a mouse model. (Doctoral dissertation). George Mason University.

Deacon, R. M. J., Brook, R. C., Meyer, D., Haeckel, O., Ashcroft, F. M., Miki, T., Seino, S. & Liss, B. (2006). Behavioral phenotyping of mice lacking the K ATP channel subunit Kir6. 2. *Physiology & behavior*, *87*, 723-733.

Finnie, J. W. & Blumbergs, P. C. (2002). Traumatic brain injury. *Veterinary Pathology, 36,* 679-689.

Gabbita, S. P., Scheff, S. W., Menard, R. M., Roberts, K., Fugaccia, I., & Zemlan, F. P. (2005). Cleaved-tau: A biomarker of neuronal damage after traumatic brain injury. *Journal of Neurotrauma, 22*(1), 83-64.

Gervase, T. (2019). Instinctual behaviors in double transgenic young adult mice are impaired following repetitive mild TBI. *Society for Neuroscience,* Abstract.

Ghajar, J. (2000). Traumatic brain injury. *The Lancet, 356,* 923-929.

Hall, A. M. & Roberson, E. D. (2012). Mouse models of Alzheimer's disease. *Brain Research Bulletin, 88,* 3-12.

Hardy, J. (2002). The relationship between amyloid and tau. *Journal of Molecular Neuroscience, 20,* 203-206.

Iliff, J. J., Chen, M. J., Plog, B. A., Zeppenfeld, D. M., Soltero, M., Yang, L., Singh, I., Deane, R., & Nedergaard, M. (2014). Impairment of glymphatic pathway function promotes tau pathology after traumatic brain injury. *The Journal of Neuroscience, 49,* 16180-16193.

Iqbal, K., Alonso, A. C., Chen, S., Chohan, M. O., El-Akkad, E., Gong, C. X., Khatoon, S., Li, B., Liu, B., Rahman, A., Tanimukai, H., & Grundke-Iqbal, I. (2005). Tau pathology in Alzheimer's disease and other taupoathies. *Molecular Basis of Disease, 1739*(2), 198-210.

Khachaturian, Z. S. (1985). Diagnosis of Alzheimer's disease. *Arch Neurology, 42,* 1097-1105.

Kochen, W. R. (2019). The effect of chronic variable stress on repetitive mild traumatic brain injury with intranasal zinc treatment. (Doctoral dissertation). George Mason University.

Lewis, J., McGowan, E., Rockwood, J., Melrose, H., Nacharaju, P., Van Slegtenhorst, M., Gwinn-Hardy, K., Murphy, M. P., Baker, M., Yu, X., Duff, K., Hardy, J., Corral, A., Lin, W. L., Yen, S. H., Dickson, D. W., Davies, P., & Hutton, M. (2000). Neurofibrillary tangles, amyotrophy and progressive motor disturbance in mice expressing mutant (P301L) tau protein. *Nature Genetics, 25,* 402-205.

Lippi, S. L. P., Smith, M. L., & Flinn, J. M. (2018). A novel hAPP/htau mouse model of Alzheimer's disease: inclusion of APP with tau exacerbates behavioral deficits and zinc administration heightens tangle pathology. *Frontiers in Aging Neuroscience, 10,* 382.

Mattson, M. P., Guo, Q., Furukawa, K., Pedersen, W. A. (1998). Presenilins, the endoplasmic reticulum, and neuronal apoptosis in Alzheimer's disease. *Journal of Neurochemistry, 70,* 1-14.

Mizukami, K., Akatsu, H., Abrahamson, E. E., Mi, Z., & Ikonomovic, M. D. (2015). Immunohistochemical analysis of hippocampal butyrylcholinesterase: Implications for reginal vulnerability in Alzheimer's disease. *Neuropathology, 36,* 135-145.

Moir, R. D., Lathe, R., Tanzi, R. E. (2018). The antimicrobial protection hypothesis of Alzheimer's disease. *Alzheimer's and Dementia, 14,* 1602-1614.

Mucke, L., Masliah, E., Yu, G., Mallory, M., Rockenstein, E. M., Tatsuno, G., Hu, K., Kholodenko, D., Johnson-Wood, K., & McConlogue, L. (2000). High-level neuronal expression of $A\beta_{1-42}$ in wildtype human amyloid protein precursor transgenic mice: Synaptotoxicity without plaque formation. *The Journal of Neuroscience, 20,* 4050-4058.

Noble, W., Hanger, D. P., Miller, C. C. J., & Lovestone, S. (2013). The importance of tau phosphorylation for neurodegenerative diseases. *Frontiers in Neurology, 4,* 1-11.

O'Brien, R. J. & Wong, P. C. (2011). Amyloid precursor protein processing and Alzheimer's disease. *Annual Review of Neuroscience, 34,* 185-204.

Oddo, S., Caccamo, A., Shepherd, J. D., Murphy, M. P., Golde, T. E., Kayed, R., Metherate, R., Mattson, M. P., Akbari, Y., & LaFerla, F. M. (2003). Triple-transgenic model of Alzheimer's disease with plaques and tangles: intracellular Aβ and synaptic dysfunction. *Neuron, 39,* 409-421.

Ojo, J. O., Mouzon, B., Greenberg, M. B., Bachmeier, C., Mullan, M., & Crawford, F. (2013). Repetitive mild traumatic brain injury augments tau pathology and glial

activation in aged htau mice. *Journal of Neuropathology and Experimental Neurology, 72,* 137-151.

Ramsden, M., Kotilinek, L., Forster, C., Paulson, J., McGowan, E., SantaCruz, K., Guimaraes, A., Yue, M., Lewis, J., Carlson, G., Hutton, M., Ashe, K. H. (2005). Age-dependent neurofibrillary tangle formation, neuron loss, and memory impairment in a mouse model of human tauopathy (P301L). *The Journal of Neuroscience, 46,* 10637-10647.

Roberson, E. D., Halabisky, B., Yoo, J. W., Yao, J., Yan, F., Wu, T., Hamto, P., Devidze, N., Yu, G. Q., Palop, J. J., Noebels, J. L., & Mucke, L. (2011). Amyloid- β/Fyn-induced synaptic, network, and cognitive impairments depend on tau levels in multiple mouse models of Alzheimer's disease. *The Journal of Neuroscience, 2,* 700-711.

Sivanandam, T. M. & Thakur, M. K. (2012). Traumatic brain injury: A risk factor for Alzheimer's disease. *Neuroscience and Biobehavioral Reviews, 36,* 1376-1381.

Small, S. A. & Duff, K. (2008). Linking Aβ and tau in late-onset Alzheimer's disease: A dual pathway hypothesis. *Neuron, 60,* 534-542.

Spires, T. L., Orne, J. D., SantaCruz, K., Pitstick, R., Carlson, G. A., Ashe, K. H., & Hyman, B. T. (2006). Region-specific dissociation of neuronal loss and neurofibrillary pathology in a mouse model of tauopathy. *American Journal of Psychology, 168,* 1598-1607.

Steinhilb, M. L., Dias-Santagata, D., Filga, T. A., Felch, D. L., & Feany, M. B. (2007). Tau phosphorylation sites work in concert to promote neurotoxicity in vivo. *Molecular Biology of the Cell, 18,* 5060-5068.

Sobol, A., Galluzzo, P., Liang, S., Rambo, B., Skucha, S., Weber, M. J., Alani, S., Bocchetta, M. (2014). Amyloid precursor protein (APP) affects global protein synthesis in dividing human cells. *Journal of Cellular Physiology, 230,* 1064-1074.

Tran, H., Brody, D. L., Bateman, R., Diamond, M., Gidday, J., Holtzman, D., & Shaw, P. (2011). The association between tramatic brain injury and Alzheimer's disease: Mouse models and potential mechanisms. *Dissertation Publishing.*

Tran, H. T., LaFerla, F. M., Holtzman, D. M., & Brody, D. L. (2011). Controlled cortical impact traumatic brain injury in 3xTg-AD mice causes acute intra-axonal amyloid-β accumulation and independently accelerates the development of tau abnormalities. *Journal of Neuroscience, 26,* 9513-9525.

Uryu, K. Laurer, H., McIntosh, T., Praticò, D., Martinez, D., Leight, S., Lee, V. M. Y., & Trojanowski, J. Q. (2002). Repetitive mild brain trauma accelerates Aβ deposition, lipid peroxidation, and cognitive impairment in transgenic mouse model of Alzheimer amyloidosis. *The Journal of Neuroscience, 2,* 446-454.

Wright, A. L., Zinn, R., Hohensinn, B., Konen, L. M., Beynon, S. B., Tan, R. P., Clark, I. A., Abdipranonto, A., & Vissel, B. (2013). Neuroinflammation and neuronal loss precede Aβ plaque deposition in the hAPP-J20 mouse model of Alzheimer's disease. *PLoS ONE, 8.*

Zempel, H., Thies, E., Mandelkow, E., & Mandelkow, E. M. (2010). Aβ oligomers caused localized Ca^{2+} elevation, missorting of endogenous tau into dendrites, tau phosphorylation, and destruction of microtubules and spines. *The Journal of Neuroscience, 36,* 11938-11950.

Zou, K., Liu, J., Watanabe, A., Hiraga, S., Liu, S., Tanabe, C., Maeda, T., Terayama, Y., Takahashi, S., Michikawa, M., & Komano, H. (2013). $Aβ_{43}$ is the earliest-depositing Aβ species in APP transgenic mouse brain and is converted to $Aβ_{41}$ by two active domains of ACE. *The American Journal of Pathology, 182,* 2322-2331.

BIOGRAPHY

Natalie Coschigano graduated from Athens High School, The Plains, Ohio, in 2013. She received her Bachelor of Arts from The College of Wooster, Wooster, Ohio, in 2017. She received her Master of Arts in Psychology from George Mason University, Fairfax, Virginia, in 2019.